

Neutrino pair emission from excited atoms

M. Yoshimura

Center of Quantum Universe and Department of Physics, Okayama University, Tsushima-naka 3-1-1, Okayama 700-8530, Japan
(Received 24 December 2006; revised manuscript received 4 April 2007; published 25 June 2007)

We explore a possibility of measuring the absolute magnitude and the nature (Majorana vs Dirac) of neutrino masses, by using a novel process of neutrino pair emission from metastable excited atoms. Except lepton number nonconserving processes, the neutrino pair ($\nu\bar{\nu}$) emission is the unique process to directly distinguish the Majorana neutrino from the Dirac neutrino, using the interference effect of identical fermions. The small energy difference between atomic levels makes it easier to measure small neutrino masses as indicated by neutrino oscillation experiments. The crucial point is how to enhance the rate of pair emission without enhancing the radiative decay. We discuss two particular cases; (1) laser irradiated pair emission from metastable atoms, and (2) microwave irradiated emission from circular Rydberg states. A new mechanism of the parametric amplification to enhance the neutrino pair emission is pointed out when Rydberg atoms are irradiated by microwave, while the radiative process may be inhibited by the cavity QED effect. A great variety of measurable neutrino parameters and a variety of experimental methods make this investigation attractive.

DOI: [10.1103/PhysRevD.75.113007](https://doi.org/10.1103/PhysRevD.75.113007)

PACS numbers: 14.60.Pq, 14.60.Lm

I. INTRODUCTION

The nature of neutrino masses, along with their precise values and their mixing parameters which appear in the weak interaction, is of fundamental importance to explore physics far beyond the standard model. In particular, whether the neutrino belongs to the special class of neutral particles described by the Majorana equation, or to the usual Dirac particle we are so familiar with, is a central issue of great interest.

In the present work we propose a novel approach to answer this important issue, the Majorana vs the Dirac particle, and suggest new experimental methods to do this. Moreover, we would like to suggest a method to simultaneously determine absolute values of neutrino masses in the same experiment.

The neutrino masses indicated by recent oscillation experiments suggest, but do not determine, the hierarchical mass pattern. One tends to take a view that two mass scales suggested by the atmospheric neutrino and the solar neutrino oscillation is close to two heavier neutrino masses, with a small correction from the lightest neutrino;

$$m_3 \sim 50 \text{ meV}, \quad m_2 \sim 10 \text{ meV}, \quad m_1 \ll m_2. \quad (1)$$

This is the case of the normal hierarchy. On the other hand, in the case of the inverted hierarchy one has the mass relation; $m_3 \approx m_2 \sim 50 \text{ meV}$, $m_3^2 - m_2^2 \sim (10 \text{ meV})^2$, $m_1 \ll m_2$. How small the lightest mass m_1 is and how much the heaviest neutrino of mass m_3 is mixed in the flavor state ν_e are both important questions unanswered by neutrino oscillation experiments so far. It is desirable for a single, well-organized experiment to be able to address all these questions. Indeed, our proposal directly attempts to answer all these problems with an extra bonus; if the method works ideally, one may hope to embark on the

neutrino mass spectroscopy, along with the determination of the Majorana vs Dirac particle.

Available energy difference between atomic levels is closest to small neutrino masses indicated by neutrino oscillation. Other energy scales are much larger; for instance the tritium beta endpoint $\sim 18.6 \text{ keV}$. Among others, Rydberg states [1] of a large principal quantum number n have energy difference to nearest levels of order,

$$\Delta E \sim 27 \text{ meV} \Delta n \left(\frac{n}{10} \right)^{-3}. \quad (2)$$

This makes it urgent to seriously consider atomic experiments for the neutrino mass measurement, if the rate lies within the experimental reach. The pair emission rate scales with $G_F^2 E^5$ with the energy E , the constant being the Fermi coupling $G_F \sim 10^{-5} \text{ GeV}^{-2}$, hence it is usually impossible to have a reasonable rate, unless some novel mechanism of enhancement is proposed.

In the present work we discuss two different types of enhanced atomic transitions; $\gamma + I^* \rightarrow I^{**} + \nu_i \nu_j$, where γ is either a laser photon or a microwave photon. The initial atomic state I^* is a metastable excited state of a long lifetime, for instance $> 1 \text{ sec}$, while the final state I^{**} has a strong E1 rate to a lower level such as the ground state. The experimental signal would be a detection of transition to the level I^{**} experimentally designed vacant initially. For unambiguous identification of a weak interaction process such as this neutrino pair emission it is desirable to measure a parity violating quantity such as the rate difference between initial different circular polarizations. In the first case of laser irradiated pair emission, one uses a resonance effect for enhancement. Our second, and a more ambitious proposal is to utilize an inherent instability and its associated enhanced decay of neutrino pair emission when Rydberg states are irradiated by a strong microwave field, at the same time using the princi-

ple of inhibition of ordinary radiative decay in a microwave cavity, a cavity QED effect [2].

The laser irradiated pair emission, perhaps using a more conventional experimental technique, might be the shortest route towards establishing the largest mass m_3 and the distinction of Majorana and Dirac neutrino. The Rydberg atom may lead to a more complete neutrino spectroscopy, including a precision determination of smaller masses and mixing angles.

To the best of our knowledge the neutrino pair emission from atomic excited states, either spontaneous or photon initiated, has not been observed so far, or even not discussed extensively in the literature, presumably due to a clear lack of interest. We wish to point out here that the atomic pair emission is ideal for a precision neutrino spectroscopy.

The rest of the paper is organized as follows.

In Sec. I we describe in detail how to distinguish the Majorana and the Dirac neutrinos. Our approach uses the 2-component formalism for both cases of the Majorana and the Dirac fields. Neutrinos that participate in the standard weak interaction of the $SU(3) \times SU(2) \times U(1)$ gauge theory are described by chirally projected 2-component spinors. We find it most unambiguous and straightforward to use the 2-component spinor both for neutrinos and electrons under the nuclear Coulomb field, in order to clarify and unambiguously identify the true nature of massive Majorana neutrino. This is done using a representation of 4×4 gamma matrices as given in Appendix A, which is not the most popular one in the literature, but is explained in many textbooks such as [3]. A comparison of the 2- and the 4-component approaches is also given in Ref. [3].

The most popular approach uses the 4-component spinor ψ with the Majorana condition $\psi^C = \psi$, which essentially reduces the 4-component ψ to the 2-component spinor, $\varphi \sim \psi^C + \psi$. A great merit of the 2-component formalism is that it uses independent variables alone. On the other hand, the 4-component formalism uses redundant fields constrained by the Majorana condition. We prefer to use independent components alone since the neutrino that appears in the usual weak interaction needs two components φ alone. In our 2-component approach it is made evident below that the distinction of the massive Majorana and the Dirac cases occurs only via the interference term of two identical particles present in the Majorana case.

We then present the pair $\nu\bar{\nu}$ emission amplitude and demonstrate how the distinction arises in the two cases. The other place where the Majorana nature arises might be in lepton number nonconserving processes such as the neutrinoless double beta decay. But in the case of lepton number nonconservation there can be no proof that the Majorana neutrino is directly involved, since there might be another source of lepton number nonconservation..

In Sec. II we work out kinematical factors of the pair emission from excited atoms. In Sec. III we discuss one of the enhanced processes; laser irradiated pair emission.

How the threshold behavior of photon irradiated pair emission differs in the Majorana and the Dirac neutrinos is described in detail. We then numerically estimate the rate for this process assuming a standard laser flux of commercially available frequency resolution. We shall further illustrate how to determine neutrino parameters including 3 mass values and the angle θ_{13} [4] if the proposed experiment becomes possible.

In Sec. IV an entirely new process of pair emission from circular Rydberg atoms is discussed. Both the standard multiphoton picture and more general effect of the parametric amplification is described. The enhancement factor of the microwave irradiation is interpreted in the multiphoton picture as the existence of a great many varieties of paths of stimulated photon emission that bridge between the initial and the final states of energy difference of order of the sum of the mass of two emitted neutrinos. The multiphoton process corresponds to the narrow band region of the parametric resonance. What is more interesting is the wide band region of the parametric amplification which is missing in the multiphoton picture, and one may expect an even larger, exponential growth of the rate. We discuss the unitarity bound on the pair emission rate in the wide band region.

Our basic assumption throughout this paper is that the standard electroweak theory correctly describes the neutrino interaction, while their small masses, either of the Majorana or of the Dirac type, are generated at a much higher energy scale than the electroweak symmetry breaking. Thus, the weak current associated with neutrinos is always taken of the $V - A$ form. We warn that introduction of the $V + A$ current may drastically change the result presented here.

Throughout this paper we use the natural unit of $\hbar = 1$ and $c = 1$, and $\alpha \sim 1/137$ and $\alpha^2 m_e/2 \sim 13.6$ eV.

II. HOW TO DISTINGUISH THE MAJORANA NEUTRINO FROM THE DIRAC NEUTRINO

The most commonly assumed method of observing the Majorana nature of neutrino masses is to discover the lepton number nonconservation, as typically exemplified by the neutrinoless double beta decay. But, this is not the unique way of detection. Another, and a more direct method is to exploit the identical particle effect of Majorana particles [5], since a Majorana particle is identical to its antiparticle.

In the nonrelativistic regime where the distinction of Majorana vs Dirac particles is expected to appear, plane-wave solutions for the Majorana and the Dirac particles might appear different, and this difference might show up in many places if momentum of neutrinos is smaller than their masses. We need a systematic way to handle the most general cases. This is the purpose of the present section. In the end we shall show that there exists a representation demonstrating wave functions common to both the

Majorana and the Dirac cases. All other representations should give equivalent results to this one.

Since a convenient account of the Majorana field, in particular, of the 2-component formalism, is missing [3], we explain in detail and give fundamental formulas related to Majorana neutrinos, in particular an explicit plane-wave solution for the massive Majorana particle. Our approach is based on the 2-component spinor, and unlike many other works, in no place do we adopt the 4-component description. This way we believe that a possible complication due to a constrained fermion field of 4-component description is avoided. We shall prove that the interference term of the antisymmetrized wave function of identical fermions is the only source of distinction of the Majorana and the Dirac neutrinos. A great merit of our 2-component approach is that this simple result is an automatic consequence of our formalism.

Fine details are relegated to Appendix A, some of which should be useful in different contexts.

A. Majorana equation

Lorentz invariance allows electrically neutral particles to be described by the 2-component spinor equation, as pointed out a long time ago by Majorana. The Majorana equation for free neutrinos is

$$(i\partial_t - i\vec{\sigma} \cdot \vec{\nabla})\varphi = im\sigma_2\varphi^*, \quad (3)$$

with m the neutrino mass. The 2-component spinor φ belongs to an irreducible representation of the Lorentz group, unlike the reducible representation of the 4-component Dirac spinor. The most salient feature of this equation is that it contains φ as well as its conjugate φ^* , thus the lepton number is violated, or more properly, one cannot define the lepton number. Unless the lepton number is violated in other places of interaction, the rate of lepton number violating processes is proportional to the square of the neutrino mass, actually some weighted average of neutrino masses squared.

The plane-wave solution to Eq. (3) is given by

$$\varphi_p(x) = e^{-ip \cdot x} \begin{pmatrix} a \\ b \end{pmatrix} + e^{ip \cdot x} \begin{pmatrix} c \\ d \end{pmatrix}, \quad (4)$$

$$\begin{pmatrix} c \\ d \end{pmatrix} = \frac{E_p - \vec{\sigma} \cdot \vec{p}}{m} (-i\sigma_2) \begin{pmatrix} a^* \\ b^* \end{pmatrix}. \quad (5)$$

Consistent quantization as discussed in Appendix A leads to the normalized operator form of the plane-wave solution written in terms of the helicity eigenstate of eigenvalue h ,

$$\begin{aligned} \varphi_{\vec{p},h}(x) &= c(\vec{p}, h) e^{-ip \cdot x} u(\vec{p}, h) \\ &+ c^\dagger(\vec{p}, -h) e^{ip \cdot x} \sqrt{\frac{E_p + hp}{E_p - hp}} (-i\sigma_2) u^*(\vec{p}, h), \end{aligned} \quad (6)$$

$$u(\vec{p}, h) = \frac{1}{2} \sqrt{\frac{E_p - hp}{pE_p(p + hp_3)}} \begin{pmatrix} p + hp_3 \\ h(p_1 + ip_2) \end{pmatrix}. \quad (7)$$

The helicity eigenstate wave function satisfies $(\vec{\sigma} \cdot \vec{p}/p)u(\vec{p}, h) = hu(\vec{p}, h)$. Quantization of the Majorana field as explained in Appendix A gives the interpretation of $c(\vec{p}, h)$ and $c^\dagger(\vec{p}, -h) = (c(\vec{p}, h))^\dagger$ as annihilation and creation operators of Majorana particles of momentum \vec{p} and helicity h .

B. Weak interaction of neutrino

We only consider weak interaction of neutrinos with electron, since our subject is the atomic weak process, hence we ignore heavier charged leptons and quarks.

The Majorana neutrino field appears only in the form of the projected 2-component spinor, $\varphi = (1 - \gamma_5)\psi/2$ in all weak processes. We shall also write down the electron field operator decomposed into the 2-component form, which must be done using the same representation of γ matrices as done for the neutrino.

It is convenient to use the Fierz transformed 4-Fermi form including both charged current (CC) and neutral current (NC) interactions;

$$\begin{aligned} \frac{G_F}{\sqrt{2}} \bar{\nu}^e \gamma_\alpha (1 - \gamma_5) \nu^e \bar{e} \gamma^\alpha (1 - \gamma_5) e - \frac{G_F}{2\sqrt{2}} \sum_i \bar{\nu}^i \gamma_\alpha (1 - \gamma_5) \\ \times \nu^i \bar{e} (\gamma^\alpha (1 - 4\sin^2\theta_W - \gamma_5)) e, \end{aligned} \quad (8)$$

where $\sin^2\theta_W \approx 0.231$ experimentally. The relative sign of CC and NC terms becomes important later.

Care must be taken of the effect of the nuclear Coulomb field on electrons. Fortunately, to orders of α and $1/m_e$, the result is simple since $(E - m_e - V)/m_e = O[\alpha^2]$ terms can be neglected. The result of the nonrelativistic limit is summarized as

$$\begin{aligned} 2\sqrt{2}G_F \times [(\nu_e^\dagger \nu_e e^\dagger e + \nu_e^\dagger \vec{\sigma} \nu_e \cdot e^\dagger \vec{\sigma} e) \\ - \frac{1}{2} \sum_i \left(\nu_i^\dagger \nu_i e^\dagger \left[1 - 4\sin^2\theta_W \left(1 + \frac{i}{m_e} \vec{\sigma} \cdot \vec{\nabla} \right) \right] e \right. \\ \left. + \nu_i^\dagger \vec{\sigma} \nu_i \cdot e^\dagger \left[\vec{\sigma} + 4\sin^2\theta_W \frac{1}{m_e} (-i\vec{\nabla} - \vec{\sigma} \times \vec{\nabla}) \right] e \right)]. \end{aligned} \quad (9)$$

This is rearranged to

$$\mathcal{H}_W = \frac{G_F}{\sqrt{2}} \sum_{ij} j_{ij}^\alpha j_{ij}^e, \quad j_{ij}^\alpha = \nu_i^\dagger \sigma^\alpha \nu_j, \quad (10)$$

$$\begin{aligned} j_{ij,0}^e &= 4e^\dagger \left(U_{ei}^* U_{ej} - \frac{\delta_{ij}}{2} (1 - 4\sin^2\theta_W) \right. \\ &\left. + 2i\delta_{ij} \frac{\sin^2\theta_W}{m_e} \vec{\sigma} \cdot \vec{\nabla} \right) e, \end{aligned} \quad (11)$$

$$j_{ij,k}^e = 4e^\dagger \left(\sigma_k \left(U_{ei}^* U_{ej} - \frac{1}{2} \delta_{ij} \right) - 2\delta_{ij} \sin^2 \theta_W \frac{(-i\vec{\nabla} - \vec{\sigma} \times \vec{\nabla})_k}{m_e} \right) e, \quad (12)$$

with $\sigma^\alpha = (1, \vec{\sigma})$.

C. Dirac neutrino and comparison with Majorana neutrino

The relation to the familiar 4-component Dirac equation is explained as follows. Using a representation of the Clifford algebra that diagonalizes γ_5 (its explicit form is given in Appendix A), the Dirac equation is decomposed into two equations for two independent 2-spinors, φ and χ ;

$$(i\partial_t - i\vec{\sigma} \cdot \vec{\nabla})\varphi = m\chi, \quad (i\partial_t + i\vec{\sigma} \cdot \vec{\nabla})\chi = m\varphi. \quad (13)$$

Thus, the identification by $\chi = i\sigma_2\varphi^*$ in the Dirac equation gives the Majorana equation, Eq. (3).

Physical content of these two equations appears different; only 2 helicity states exist for the Majorana field, a particle being identical to its antiparticle, unlike the distinguishable particle and antiparticle for the Dirac case. Whether the neutrino as observed in the $V - A$ weak interaction belongs to the Majorana case or the Dirac case is the unsettled question facing fundamental physics.

It is important to theoretically compare the chirality-projected Dirac field $\psi_D = (1 - \gamma_5)\psi/2$ to the Majorana field. The relevant 2-component operator corresponding to the momentum eigenstate $\propto e^{-iE_p t + i\vec{p} \cdot \vec{x}}$ is

$$\psi_D = b(\vec{p}, h)e^{-ip \cdot x} u(\vec{p}, h) + d^\dagger(\vec{p}, -h)e^{ip \cdot x} \sqrt{\frac{E_p + hp}{E_p - hp}} (-i\sigma_2) u^*(\vec{p}, h). \quad (14)$$

Here $u(\vec{p}, h)$ is given by Eq. (7). The antiparticle creation operator $d^\dagger(\vec{p}, h)$ appears here, which is distinct from the particle creation $b^\dagger(\vec{p}, h)$.

Comparison of the Majorana solution, Eqs. (6) and (7) and the projected Dirac solution, Eq. (14) demonstrates the equivalence of the two wave functions, the difference being the distinction of the Majorana particle c^\dagger and the Dirac antiparticle d^\dagger creation. Their distinction appears only via the identical particle effect of two Majorana fermions, an extra term containing $c_2^\dagger c_1^\dagger = -c_1^\dagger c_2^\dagger$. The unique process to distinguish the massive Majorana from the massive Dirac neutrino is thus the pair emission $\nu\bar{\nu}$, in which the antisymmetrized wave function appears only for Majorana neutrinos. We shall later show that this distinction too disappears in the high energy limit of $E_p \gg m$. On the other hand, neither a single nor a pair $\nu\nu$ (not $\nu\bar{\nu}$) emission can tell their distinction even for nonrelativistic massive neutrinos, although they may be able to determine the absolute mass of neutrinos. In this sense the double beta

decay of two accompanying neutrinos $\nu_e\nu_e$ is useless for distinction of the Majorana and the Dirac neutrino. There are thus only two experimental ways to verify the Majorana nature of neutrinos; the other indirect method is to verify the lepton number nonconservation such as in the neutrinoless double beta decay.

D. Pair emission

The idea of using the decay of unstable elementary particles to verify the Majorana nature of neutrinos via identical particle effects is not new; for instance, see [5,6]. The problem of this approach is a huge disparity of energy scales; in both cases of the rare K -meson decay $K \rightarrow \pi + \nu_i\nu_j$ [5] and the muon decay $\mu^+ \rightarrow e^+ \nu_e \bar{\nu}_\mu$ [6], the mass difference is much larger than anticipated neutrino masses, and even if events of this process are accumulated statistically, there is no sensible way to precisely determine the neutrino mass.

On the other hand, the atomic energy difference is closer to the neutrino mass scale;

$$\Delta E_{n_1, n_2} \sim 13.6 \text{ eV} \times \left(\frac{1}{n_2^2} - \frac{1}{n_1^2} \right) \quad (15)$$

which reduces to $27 \text{ meV} \Delta n / (n/10)^3$ for $|n_1 - n_2| \sim n \gg 1$ for Rydberg states.

Let us first discuss the neutrino pair $\nu_2 \bar{\nu}_1$ emission of Dirac particles. Note that the antiparticle notation $\bar{\nu}_1$ is necessary only for the Dirac case. The Dirac pair emission $\propto b^\dagger(\vec{p}_2, h_2) d^\dagger(\vec{p}_1, h_1)$ is governed by $e^{i(\vec{p}_1 + \vec{p}_2) \cdot \vec{x}}$ times the current matrix element,

$$j_D^\alpha(\vec{p}_1 h_1, \vec{p}_2 h_2) = -\sqrt{\frac{E_1 + h_1 p_1}{E_1 - h_1 p_1}} u^\dagger(\vec{p}_2, -h_2) \times \sigma^\alpha i\sigma_2 u^*(\vec{p}_1, h_1). \quad (16)$$

The pair emission rate contains a neutrino current product;

$$j_D^\alpha (j_D^\beta)^\dagger = \frac{1}{16} \left(1 + h_2 \frac{p_2}{E_2} \right) \left(1 + h_1 \frac{p_1}{E_1} \right) \text{tr} \left(1 - h_2 \frac{\vec{\sigma} \cdot \vec{p}_2}{p_2} \right) \times \sigma^\alpha \left(1 - h_1 \frac{\vec{\sigma} \cdot \vec{p}_1}{p_1} \right) \vec{\sigma}^\beta, \quad (17)$$

with $\vec{\sigma}^\beta = (1, -\vec{\sigma})$.

The neutrino pair current given above is to be multiplied by the electron current product. After this multiplication, the helicity summed quantity for the Dirac case is

$$\begin{aligned}
\sum_{h_1 h_2} |j_D \cdot j^e|^2 &= \frac{1}{2} \left(\left(1 + \frac{\vec{p}_1 \cdot \vec{p}_2}{E_1 E_2} \right) j_0^e (j_0^e)^\dagger + \left(1 - \frac{\vec{p}_1 \cdot \vec{p}_2}{E_1 E_2} \right) \right. \\
&\quad \times \tilde{j}^e (\tilde{j}^e)^\dagger + 2 \Re \frac{\vec{p}_1 \cdot \tilde{j}^e \vec{p}_2 \cdot (\tilde{j}^e)^\dagger}{E_1 E_2} \\
&\quad - 2 \left(\frac{\vec{p}_1}{E_1} + \frac{\vec{p}_2}{E_2} \right) \cdot \Re j_0^e (\tilde{j}^e)^\dagger + 2 \frac{\vec{p}_1 \times \vec{p}_2}{E_1 E_2} \\
&\quad \cdot \Im j_0^e (\tilde{j}^e)^\dagger + 2 \left(\frac{\vec{p}_1}{E_1} - \frac{\vec{p}_2}{E_2} \right) \cdot \Re \tilde{j}^e \times \Im \tilde{j}^e \left. \right). \quad (18)
\end{aligned}$$

The last two quantities in proportion to imaginary parts of the current product may contain CP -odd effects.

Let us next discuss the Majorana pair emission. The Majorana pair emission operator, $c^\dagger(\vec{p}_2, h_2) c^\dagger(\vec{p}_1, h_1)$, gives a matrix element of two antisymmetrized wave functions due to the anticommutation of the Majorana field. The neutrino current for the pair emission is thus $e^{i(\vec{p}_1 + \vec{p}_2) \cdot \vec{x}}$ times

$$\begin{aligned}
j_M^\alpha(\vec{p}_1 h_1, \vec{p}_2 h_2) &= -i \sqrt{\frac{E_2 - h_2 p_2}{E_2 + h_2 p_2}} u^\dagger(\vec{p}_1, h_1) \\
&\quad \times \sigma^\alpha \sigma_2 u^*(\vec{p}_2, -h_2) \\
&\quad + i \sqrt{\frac{E_1 + h_1 p_1}{E_1 - h_1 p_1}} u^\dagger(\vec{p}_2, -h_2) \\
&\quad \times \sigma^\alpha \sigma_2 u^*(\vec{p}_1, h_1). \quad (19)
\end{aligned}$$

To derive the rate, one multiplies the electron current j_e^α and takes its square. After a little algebra, one finds for the relevant quantity of the neutrino part,

$$\begin{aligned}
j_M^\alpha (j_M^\beta)^\dagger &= \frac{1}{16} \left(1 + h_1 \frac{p_1}{E_1} \right) \left(1 + h_2 \frac{p_2}{E_2} \right) \times \text{tr} \left(1 - h_2 \frac{\vec{\sigma} \cdot \vec{p}_2}{p_2} \right) \\
&\quad \times \sigma^\alpha \left(1 - h_1 \frac{\vec{\sigma} \cdot \vec{p}_1}{p_1} \right) \tilde{\sigma}^\beta + (1 \leftrightarrow 2) \quad (20) \\
&\quad + \frac{m_1 m_2}{16 E_1 E_2} \text{tr} \left(1 - h_2 \frac{\vec{\sigma} \cdot \vec{p}_2}{p_2} \right) \\
&\quad \times \sigma^\alpha \left(1 - h_1 \frac{\vec{\sigma} \cdot \vec{p}_1}{p_1} \right) \sigma^\beta + (1 \leftrightarrow 2). \quad (21)
\end{aligned}$$

The last two terms of Eq. (21) are the interference terms proper to identical fermions.

It is evident that without the interference terms $\propto m_1 m_2 / (E_1 E_2)$ in (21), the Dirac and the Majorana emission rates are identical, by considering an extra factor 1/2 for the Majorana case, which is necessary after the phase space integration because the same configuration of identical particles are counted twice. Hereafter we divide the Majorana contribution by 2, anticipating this overcounting beforehand.

The helicity summed interference term thus becomes

$$\frac{m_1 m_2}{2 E_1 E_2} (j_0^e (j_0^e)^\dagger - \tilde{j}^e \cdot (\tilde{j}^e)^\dagger). \quad (22)$$

Hence the current product in the rate for the Majorana emission is

$$\sum_{h_1 h_2} |j_M \cdot j^e|^2 = \sum_{h_1 h_2} |j_D \cdot j^e|^2 + \frac{m_1 m_2}{2 E_1 E_2} (j_0^e (j_0^e)^\dagger - \tilde{j}^e \cdot (\tilde{j}^e)^\dagger). \quad (23)$$

The interference term is CP even. Hence the CP violating effect is identical in the Dirac and the Majorana cases, for the neutrino pair emission.

As an illustration, let us work out the current product by neglecting $1/m_e$ terms and taking $\sin^2 \theta_W = 1/4$. We call this the leading approximation of $1/m_e$ expansion. The spin and the orbital part of the electron current is separated as

$$j_0^e = \delta_{ss'} a_{if}(\vec{p}_1 + \vec{p}_2) c_{ij}^{(0)}, \quad (24)$$

$$\tilde{j}^e = \langle s' | \vec{\sigma} | s \rangle a_{if}(\vec{p}_1 + \vec{p}_2) c_{ij}^{(s)},$$

$$a_{if}(\vec{p}_1 + \vec{p}_2) = \langle f | e^{-i(\vec{p}_1 + \vec{p}_2) \cdot \vec{x}} | i \rangle, \quad (25)$$

$$c_{ij}^{(0)} = U_{ei}^* U_{ej}, \quad c_{ij}^{(s)} = U_{ei}^* U_{ej} - \frac{1}{2} \delta_{ij}. \quad (26)$$

Furthermore, we consider the spin averaged rate such that

$$\frac{1}{2} \sum_{ss'} j_k^e (j_l^e)^\dagger = \delta_{kl} |a_{if}(\vec{p}_1 + \vec{p}_2)|^2 |c_{ij}^{(s)}|^2,$$

$$\frac{1}{2} \sum_{ss'} j_0^e (j_0^e)^\dagger = |a_{if}(\vec{p}_1 + \vec{p}_2)|^2 |c_{ij}^{(0)}|^2.$$

The result of the spin average for the Dirac and the Majorana cases is

$$\begin{aligned}
\frac{1}{2} \sum_{ss'} \sum_{h_1 h_2} |j_D \cdot j^e|^2 &= |a_{if}(\vec{p}_1 + \vec{p}_2)|^2 \frac{1}{2} \left(\left(1 + \frac{\vec{p}_1 \cdot \vec{p}_2}{E_1 E_2} \right) |c_{ij}^{(0)}|^2 \right. \\
&\quad + \left(3 - \frac{\vec{p}_1 \cdot \vec{p}_2}{E_1 E_2} \right) |c_{ij}^{(s)}|^2 \\
&\quad \left. + 2 \left(\frac{\vec{p}_1}{E_1} - \frac{\vec{p}_2}{E_2} \right) \cdot \text{Re} \tilde{j}^e \times \Im \tilde{j}^e |c_{ij}^{(s)}|^2 \right), \quad (27)
\end{aligned}$$

$$\begin{aligned}
\frac{1}{2} \sum_{ss'} \sum_{h_1 h_2} |j_M \cdot j^e|^2 &- \frac{1}{2} \sum_{ss'} \sum_{h_1 h_2} |j_D \cdot j^e|^2 \\
&= -|a_{if}(\vec{p}_1 + \vec{p}_2)|^2 \frac{m_1 m_2}{2 E_1 E_2} (3 |c_{ij}^{(s)}|^2 - |c_{ij}^{(0)}|^2). \quad (28)
\end{aligned}$$

The long wavelength approximation for the neutrino makes this formula much simpler, allowing the replacement

$$|a_{if}(\vec{p}_1 + \vec{p}_2)|^2 = |\langle f | e^{-i(\vec{p}_1 + \vec{p}_2) \cdot \vec{x}} | i \rangle|^2 \rightarrow 1. \quad (29)$$

This is valid if the wavelength of the neutrino $\lambda_\nu \gg$ atomic size, or $p_\nu \ll Z \alpha m_e / n^2$. Since our main interest

is in the region of the neutrino mass, this means, with $m_\nu \leq p_\nu$,

$$m_\nu \ll \frac{Z\alpha m_e}{n} \sim 3.7 \text{ keV} \frac{Z}{n^2}. \quad (30)$$

This relation holds in the following discussion for laser irradiated process, but may not for pair emission from Rydberg atoms. The condition for the long wavelength approximation is significantly modified for Rydberg atoms.

III. KINEMATICS OF PAIR DECAY

A. What can be measured from the pair decay

A merit of the process of neutrino pair emission from excited atoms is a great variety of measurable quantities related to the neutrino mass parameter. The neutrino pair $\nu_i \nu_j$ can be any combination ij of mass eigenstates, as is clear from the coexistence of the charged and the neutral current interaction. From the energy threshold position one can determine a combination of the neutrino mass $m_i + m_j$, while the strength of the rate gives the mixing parameter in the form $|U_{ei}^* U_{ej}|$. Since any pair ij (altogether 6 channels) is conceivable, there is a great many combinations. This is why we phrased our experimental approach as the Mneutrino spectroscopy. The situation is quite different from the neutrinoless double beta decay in which one concentrates only on a combination of parameters $|\sum_i U_{ei} U_{ei} m_i^2|$, which however attempts to discover the important issue of lepton number violation.

Ideally, one can determine all masses m_i with a bonus of experimental redundancy. In particular, we would like to emphasize that this is the first opportunity to probe the smallest mass m_1 . Furthermore, we may explore a possibly very small mixing factor $|U_{e3}|$, which indicates how much the heaviest neutrino is mixed in the flavor ν_e . Both are important since other experimental methods may have no good handle on these quantities.

B. Phase space factor

When the pair emission occurs between 2 levels of energy difference Δ , the rate is given by the phase space factor of 2 massive neutrinos $\nu_i \nu_j$. The rate is

$$\Gamma_{ij}^{M,D}(\Delta) = 8G_F^2 \int \frac{d^3 q_1 d^3 q_2}{(2\pi)^5} \delta(E_1 + E_2 - \Delta) \times \frac{1}{2} \sum_{ss'} \sum_{h_1 h_2} |c_{ij} j_{M,D} \cdot j^e|^2. \quad (31)$$

The constant c_{ij} 's are different, depending on whether the electron transition involves spin-flip (F) or no flip (NF). They are in the leading $1/m_e$ approximation,

$$c_{ij} = c_{ij}^{(s)} = U_{e_i}^* U_{e_j} - \frac{\delta_{ij}}{2} \quad (\text{F}), \quad (32)$$

$$c_{ij} = c_{ij}^{(0)} = U_{e_i}^* U_{e_j} \quad (\text{NF}),$$

$$\sum_{ij} |c_{ij}^{(s)}|^2 = \frac{3}{4}, \quad \sum_{ij} |c_{ij}^{(0)}|^2 = 1. \quad (33)$$

The kinematical factor is defined, when the matrix element is ignored, as

$$f_{ij}^{(1)}(\Delta) = \int \frac{d^3 q_1 d^3 q_2}{(2\pi)^5} \delta(E_1 + E_2 - \Delta) = \frac{1}{2\pi^3} \int_{m_i}^{\Delta - m_j} dE_1 E_1 (\Delta - E_1) \times [(E_1^2 - m_i^2)((\Delta - E_1)^2 - m_j^2)]^{1/2}. \quad (34)$$

Near the threshold $\Delta \approx m_i + m_j$

$$f_{ij}^{(1)}(\Delta) \approx \frac{1}{8\pi^2} (m_i m_j)^{3/2} (\Delta - m_i - m_j)^2. \quad (35)$$

Note that the distinction of Majorana and Dirac particles appears only when $i = j$, since with $i \neq j$ two neutrinos have different masses and are not identical particles.

For illustration we shall give the rate near the threshold in the leading approximation of $1/m_e$, further suppressing the correlation of electron transition amplitude with neutrino momenta,

$$\Gamma_{ij}^M(\Delta) \approx \frac{G_F^2}{8\pi^2} |c_{ij}^{(0)}|^2 (m_i m_j)^{3/2} (\Delta - m_i - m_j)^2, \quad (36)$$

$$\Gamma_{ij}^D(\Delta) \approx \frac{G_F^2}{16\pi^2} (|c_{ij}^{(0)}|^2 + 3|c_{ij}^{(s)}|^2) (m_i m_j)^{3/2} (\Delta - m_i - m_j)^2. \quad (37)$$

IV. LASER IRRADIATED PAIR DECAY

The weak rate scales with the available energy as E^5 . This means that for a small available energy the rate is very small. For the case of the neutrino pair emission from excited atoms, the phase space factor is

$$\frac{G_F^2 E^5}{15\pi^3} \sim 3.3 \times 10^{-34} \text{ s}^{-1} \left(\frac{E}{\text{eV}}\right)^5, \quad (38)$$

which should be multiplied by the matrix element squared. One clearly needs some enhancement mechanism even to hope for detectability of the neutrino pair emission. We shall discuss in this section laser irradiated pair emission using a resonance effect.

Let us first estimate very crudely how much enhancement may be expected for resonant processes. Suppose that the neutrino pair emission from a metastable atom of lifetime $1/\gamma$ is triggered by laser irradiation of flux F_0 . The rate for photon absorption is σF_0 with σ the photo-

absorption cross section, and this irradiation is effective for the duration of the lifetime. Putting these factors together, one might naively expect a laser irradiated rate of order, $\sigma F_0 \Gamma_{\nu\bar{\nu}}/\gamma$, with $\Gamma_{\nu\bar{\nu}}$ the rate of order (38).

Another important factor is the energy resolution $\Delta\omega$ of the laser. Convolution of the laser spectral function with the Breit-Wigner resonance function of the natural width γ leads to a factor of order

$$\frac{\omega_0^2}{\gamma\Delta\omega} = 1.5 \times 10^{24} \frac{10^{-9}\omega_0}{\Delta\omega} \frac{\omega_0}{1 \text{ eV}} \frac{1 \text{ s}^{-1}}{\gamma}, \quad (39)$$

with ω_0 the laser central frequency. It was assumed that $\Delta\omega \gg \gamma$, which is usually valid. We shall take a standard laser flux of order

$$F_0 = \frac{Wmm^{-2}}{\text{eV}} \approx 6.2 \times 10^{20} \text{ cm}^{-2} \text{ sec}^{-1} \\ \approx 1.6 \times 10^{-4} (\text{eV})^3, \quad (40)$$

and the photo-absorption cross section of order nm^2 . The laser beam power P is related to the number flux F_0 by $P = \omega_0 F_0$, with $\omega_0 = \hbar \times$ the laser frequency.

This leads to a typical laser irradiated rate of order

$$\frac{G_F^2 E^5}{15\pi^3} \frac{\omega_0 \sigma F_0}{\Delta\omega \gamma} \sim 2 \times 10^{-18} \text{ s}^{-1} \frac{1 \text{ s}^{-1}}{\gamma} \frac{\sigma}{nm^2} \left(\frac{E}{1 \text{ eV}} \right)^5 \\ \times \left(10^{-9} \frac{\omega_0}{\Delta\omega} \right) \frac{P}{Wmm^{-2}}. \quad (41)$$

In the following we shall give a more concrete estimate for a particular process of laser irradiated pair emission.

We consider [7] laser irradiated neutrino pair emission from metastable ions or atoms $|I^*\rangle$,

$$\gamma + I^* \rightarrow I^{**} + \nu_i \nu_j, \quad (42)$$

where the final state $|I^{**}\rangle$ is a short-lived excited state, as depicted in Fig. 1 [8]. Detection of $|I^{**}\rangle$, presumably via radiative decay into the ground state, gives a signature of this weak process. A measurement of parity violating quantity is highly desirable for the background rejection.

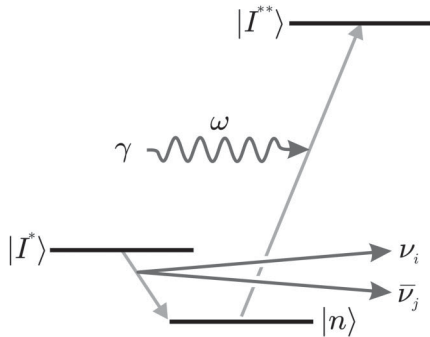


FIG. 1. Atomic level structure and laser irradiated neutrino pair emission.

The intermediate state $|I^n\rangle$ is chosen to lie energetically below the initial state $|I^*\rangle$ by an amount of the paired neutrino energy $E_i + E_j$ with $E_i = \sqrt{\vec{p}_i^2 + m_i^2}$. The laser frequency is tuned to the next step of radiative transition from $|I^n\rangle$ to the final state $|I^{**}\rangle$. The Breit-Wigner resonance factor

$$\frac{1}{(E_* - E_n - E_i - E_j)^2 + \gamma^2/4} \\ = \frac{1}{(E_{**} - E_n - \omega)^2 + \gamma^2/4}, \quad (43)$$

with the energy conservation $E_* + \omega = E_{**} + E_i + E_j$, gives a large enhancement at the threshold $E_i + E_j = m_i + m_j$, if

$$E_n \approx E_* - m_i - m_j, \quad \omega \approx E_{**} - E_* + m_i + m_j. \quad (44)$$

Thus the laser initiated pair emission has the threshold at the laser energy of

$$\omega_{\text{th}} = E_{**} - E_* + m_i + m_j. \quad (45)$$

The threshold location ω_{th} is expected to be measured with a good precision of the laser frequency.

The initial state $|I^*\rangle$ must be a metastable excited state, for instance $O[2m_3]$ above another state $|I^n\rangle$. The intermediate state $|I^n\rangle$ can be either a ground state, or better, another metastable state. The width factor given by $\gamma^2 = \gamma_*^2 + \gamma_n^2$ is a sum of the initial and the intermediate state contributions. We assume that both of these widths are of order 1 sec^{-1} or smaller. There are many candidate atoms or ions of this kind. Another important assumption is that we prepare depletion of the intermediate state $|I^n\rangle$, since the laser excitation of this state to $|I^{**}\rangle$ is the crucial signature of the pair emission process.

To lowest order of the weak interaction, the rate for the pair emission $\nu_i \nu_j$ of mass eigenstates when a laser of flux $F(\omega)$ is irradiated, is given by

$$\Gamma_{ij}^{M,D}(\omega) = F(\omega) \frac{8G_F^2 e^2 \omega |\langle I^{**} | \vec{x} | I^n \rangle|^2}{3[(\omega - \Delta_{fn})^2 + \gamma^2/4]} f_{ij}^{M,D}(\omega - \Delta_{fi}), \quad (46)$$

$$2f_{ij}^D(\Delta) = f_{ij}^{(1)}(\Delta)(|c_{ij}^{(0)}|^2 + 3|c_{ij}^{(s)}|^2), \quad (47)$$

$$2f_{ij}^M(\Delta) - 2f_{ij}^D(\Delta) = f_{ij}^{(2)}(\Delta)(|c_{ij}^{(0)}|^2 - 3|c_{ij}^{(s)}|^2), \quad (48)$$

$$f_{ij}^{(2)}(\Delta) = \int \frac{d^3 q_1 d^3 q_2}{(2\pi)^5} \delta(E_1 + E_2 - \Delta) \frac{m_i m_j}{E_1 E_2}, \quad (49)$$

where $f_{ij}^{(1)}$ is defined by (34), and

$$\Delta_{fn} = E_{**} - E_n, \quad \Delta_{fi} = E_{**} - E_*. \quad (50)$$

The Majorana and the Dirac difference $\propto f_{ij}^{(2)}(\omega - \Delta_{fi}) \times (|c_{ij}^{(0)}|^2 - 3|c_{ij}^{(s)}|^2)$.

When integrated over a laser spectral function of the energy resolution $\Delta\omega \gg \gamma$,

$$\int d\omega \frac{F(\omega)}{(\omega - \Delta)^2 + \gamma^2/4} \sim \frac{2\pi F_0}{\gamma\Delta\omega}, \quad (51)$$

the rate is

$$\Gamma_{ij}^M(\omega) = \frac{64\pi^2 \alpha G_F^2}{3} \frac{\omega |\langle \vec{x} \rangle|^2 F_0}{\gamma\Delta\omega} f_{ij}^M(\omega - \Delta_{fi}). \quad (52)$$

The dipole strength is related to the natural width,

$$\gamma_r = \frac{4\alpha}{3} \omega^3 |\langle \vec{x} \rangle|^2, \quad (53)$$

which gives

$$\begin{aligned} \Gamma_{ij}^M(\omega_0) &= \frac{16\pi^2 G_F^2 \gamma_r F_0}{\omega_0^2 \gamma \Delta\omega} f_{ij}^M(\omega_0 - \Delta_{fi}) \\ &= 16\pi^2 G_F^2 \frac{F_0}{\omega_0^2 \Delta\omega} \frac{\gamma_r}{\gamma} f_{ij}^M(\omega_0 - \Delta_{fi}). \end{aligned} \quad (54)$$

We assume that the laser tuning is complete. In this last formula three factors are separated; the laser quality factor $F_0/(\omega_0^2 \Delta\omega)$, the atomic factor γ_r/γ , and the neutrino kinematical factor f_{ij}^M .

Near the threshold, denoting the tuned frequency ω_0 by ω ,

$$f_{ij}^M(\omega - \Delta_{fi}) = \frac{1}{8\pi^2} |c_{ij}^{(0)}|^2 (m_i m_j)^{3/2} (\omega - \Delta_{fi} - m_i - m_j)^2, \quad (55)$$

$$\begin{aligned} f_{ij}^D(\omega - \Delta_{fi}) &= \frac{1}{16\pi^2} (3|c_{ij}^{(s)}|^2 + |c_{ij}^{(0)}|^2) (m_i m_j)^{3/2} \\ &\times (\omega - \Delta_{fi} - m_i - m_j)^2. \end{aligned} \quad (56)$$

To compute a reference rate let us take 13/4 for the asymptotic value of the factors of $|c_{ij}|^2$, which gives a basic unit of the rate

$$\begin{aligned} \frac{13}{64\pi^2} \frac{G_F^2 F_0 \gamma_r}{\omega^2 \Delta\omega \gamma} (\text{eV})^5 &= 5.0 \times 10^{-19} \text{ s}^{-1} \frac{P}{W m m^{-2}} \left(\frac{\text{eV}}{\omega}\right)^4 \\ &\times \frac{10^{-9} \omega}{\Delta\omega} \frac{10^{-9} \gamma_r}{\gamma}. \end{aligned} \quad (57)$$

We have in mind radiative rates of order, $1/\gamma_r \sim 1$ ns and $1/\gamma \sim 1$ s. Taking the energy scale at 0.3 eV, about 3 times the pair mass of the heaviest neutrino 50 meV, then gives the rate of order

$$1 \times 10^{-21} \text{ s}^{-1} \frac{f_{ij}^M(\omega)}{(0.3 \text{ eV})^5} \frac{P}{W m m^{-2}} \left(\frac{\text{eV}}{\omega}\right)^4 \frac{10^{-9} \omega}{\Delta\omega} \frac{10^{-9} \gamma_r}{\gamma}. \quad (58)$$

This corresponds to ≈ 1 event/day for 10^{16} target atoms. With a more experimental effort of improvement such as the use of the resonator for laser irradiation, an enhancement of $\approx 10^3$ – 10^4 may be expected and would help much for the improved event rate.

The threshold suppression is large due to the square factor $(\omega - \Delta_{fi} - m_i - m_j)^2$, but the rate rises towards

$$\frac{2G_F^2 \omega^5}{15\pi} (3|c_{ij}^{(s)}|^2 + |c_{ij}^{(0)}|^2) \frac{\gamma_r F_0}{\gamma \omega^2 \Delta\omega}. \quad (59)$$

This pattern repeats for each pair ij , and finally approaches at much larger $\omega \gg 2m_3$,

$$\frac{2G_F^2 \omega^5}{15\pi} \left(\frac{9}{4} + 1\right) \frac{\gamma_r F_0}{\gamma \omega^2 \Delta\omega}, \quad (60)$$

where 9/4 comes from the spin-flip term, while 1 comes from the nonflip term. To determine neutrino masses, it is necessary to fit experimental data of the threshold rise up to an intermediate energy range. It is then important to have a large statistics data with a reasonable precision in the vicinity of the threshold, typically away from the threshold a few to several times the sum $m_i + m_j$.

The neutrino mass spectroscopy may proceed step by step. First, the laser frequency dependence, for instance $\propto (\omega - \Delta_{fi} - m_i - m_j)^2$ near the threshold, may be used to determine mass parameters m_i . Simultaneous with or even prior to m_3 determination at the threshold $\nu_3 \nu_3$, distinction of the Majorana and the Dirac cases is presumably possible at $\omega - \Delta_{fi} \sim O[6m_3] \approx 0.3$ eV. Once the mass determination is done, one proceeds to determine mixing angles by measurement of the absolute rate. For instance, the sensitivity to the smallest, unknown angle θ_{13} is large at the threshold of $\omega = \Delta_{fi} + m_3 + m_1$, since the relevant factor has a large coefficient;

$$3|c_{13}^{(s)}|^2 + |c_{13}^{(0)}|^2 \sim 2.9 \sin^2 \theta_{13}. \quad (61)$$

For the hierarchical mass pattern, $m_3 + m_1 \sim 50$ meV. The rate at this threshold is smaller by a factor $\sim 1/32$ than at the threshold $2m_3 \sim 100$ meV. Although smaller in the rate, the θ_{13} measurement may be possible.

We conclude that for precision determination of absolute values of m_i , ($i = 1, 2, 3$) and θ_{13} , pair emissions of $(\nu_3 \nu_3)$, $(\nu_3 \nu_2)$, $(\nu_3 \nu_1)$ near their thresholds are channels we recommend.

A quantitative Majorana-Dirac distinction may be helped much by noting the rate difference at each threshold ij ;

$$\Gamma_{ij}^M(\omega_0) - \Gamma_{ij}^D(\omega_0) = 8\pi^2 G_F^2 \frac{\gamma_r F_0}{\gamma \omega_0^2 \Delta\omega} (|c_{ij}^{(0)}|^2 - 3|c_{ij}^{(s)}|^2), \quad (62)$$

$$|c_{ij}^{(0)}|^2 - 3|c_{ij}^{(s)}|^2 = -2|U_{ei}|^2 |U_{ej}|^2, \quad \text{for } i \neq j \quad (63)$$

$$= -2|U_{ei}|^4 + 3|U_{ei}|^2 - \frac{3}{4}, \quad \text{for } i = j. \quad (64)$$

For a reference, we give a complete rate formula including all pair channels;

$$\begin{aligned} \Gamma^M(\omega_0) &= \frac{2G_F^2 \gamma_r}{\pi^2 \omega_0^2} \int d\omega \sum_{ij} \theta(\omega - \Delta_{fi} - m_i - m_j) \\ &\times \frac{F(\omega; \omega_0, \Delta\omega)}{(\omega - \Delta_{fn})^2 + \gamma^2/4} \left[(|c_{ij}^{(0)}|^2 + 3|c_{ij}^{(s)}|^2) \right. \\ &\times (\omega - \Delta_{fi})^5 Y_{ij} \left(\frac{m_i}{\omega - \Delta_{fi}}, \frac{m_j}{\omega - \Delta_{fi}} \right) \\ &+ \delta_{ij} (|c_{ij}^{(0)}|^2 - 3|c_{ij}^{(s)}|^2) m_i m_j (\omega - \Delta_{fi})^3 \\ &\left. \times Z_{ij} \left(\frac{m_i}{\omega - \Delta_{fi}}, \frac{m_j}{\omega - \Delta_{fi}} \right) \right], \quad (65) \end{aligned}$$

$$Y_{ij}(\epsilon_i, \epsilon_j) = \int_{\epsilon_i}^{1-\epsilon_j} dx x(1-x) \sqrt{(x^2 - \epsilon_i^2)((1-x)^2 - \epsilon_j^2)}, \quad (66)$$

$$Z_{ij}(\epsilon_i, \epsilon_j) = \int_{\epsilon_i}^{1-\epsilon_j} dx \sqrt{(x^2 - \epsilon_i^2)((1-x)^2 - \epsilon_j^2)}. \quad (67)$$

We used a notation of laser spectral function $F(\omega; \omega_0, \Delta\omega)$, which has a central frequency ω_0 and an energy resolution $\Delta\omega$. In the case of the Dirac neutrino the last term $m_i m_j Z_{ij}$ in (65) is missing.

Under the assumption of $\Delta\omega \gg \gamma$, this rate becomes simplified as

$$\begin{aligned} \Gamma^M(\omega) &= \frac{4G_F^2 F_0}{\pi \omega^2 \Delta\omega} \frac{\gamma_r}{\gamma} \sum_{ij} \theta(\omega - \Delta_{fi} - m_i - m_j) \\ &\times \int_{m_i}^{\omega - \Delta_{fi} - m_j} dE_1 I(E_1), \quad (68) \end{aligned}$$

$$\begin{aligned} I(E_1) &= (|c_{ij}^{(0)}|^2 + 3|c_{ij}^{(s)}|^2) E_1 (\omega - \Delta_{fi} - E_1) \\ &\times \sqrt{(E_1^2 - m_i^2)((\omega - \Delta_{fi} - E_1)^2 - m_j^2)} \\ &+ \delta_{ij} (|c_{ij}^{(0)}|^2 - 3|c_{ij}^{(s)}|^2) m_i m_j \\ &\times \sqrt{(E_1^2 - m_i^2)((\omega - \Delta_{fi} - E_1)^2 - m_j^2)}. \quad (69) \end{aligned}$$

We plot in Fig. 2 the ratio of two rates; the Majorana rate $\Gamma^M(\omega)$ and the Dirac rate $\Gamma^D(\omega)$ divided by the rate of massless neutrino pair emission. The parameters used for this figure are

$$\begin{aligned} \sin^2 \theta_{12} &= 0.35, & \sin^2 \theta_{13} &= 0.032, \\ m_1 &= 1.0 \text{ meV}, & m_2 &= 9.0 \text{ meV}, \\ m_3 &= 50.8 \text{ meV}, \end{aligned}$$

constrained and allowed by neutrino oscillation data. With

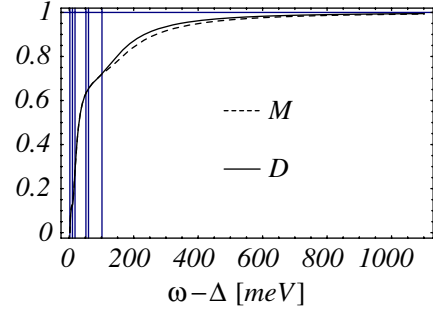


FIG. 2 (color online). Ratio of laser irradiated pair emission rate for Majorana (M) and Dirac (D) cases to the massless rate. Vertical lines indicate 6 threshold locations.

this small mass m_1 the energy region in which the Majorana rate is larger than the Dirac rate is restricted to a small region below $m_1 + m_2$. When m_1 is larger, say $m_1 \geq 2$ meV, the Majorana dominance persists up to slightly above the $2m_3$ threshold. The Majorana dominance is also sensitive to a value of $\sin^2 \theta_{12}$ [9].

These rates presented here may be an overestimate for a dense gaseous target, since the energy resolution in this case is governed by a usually much larger collisional width,

$$\gamma_{\text{coll}} \approx 1 \text{ s}^{-1} \frac{P}{10^{-7} \text{ Torr}} \sqrt{\frac{T}{300 \text{ K}}} \frac{\sigma v}{1 \text{ nm}^2}. \quad (70)$$

V. NEUTRINO PAIR EMISSION FROM CIRCULAR RYDBERG STATES

A. Circular Rydberg states

Circular Rydberg states [10] are highly excited; in addition to a large principal quantum number n , it has the highest angular momentum, $l = |m| = n - 1$. These states have the least overlap with the atomic core of charge $(Z - 1)e$. Its size $\langle r \rangle \approx n^2 a_B$ with a dispersion $\sqrt{\langle (\Delta r)^2 \rangle} \approx \sqrt{n^3/2} a_B$, and the average momentum $\langle p \rangle \approx 1/(n a_B)$ with a large dispersion. Thus, the circular Rydberg state is almost classical, and the system is approximately described by the hydrogenlike Coulomb potential of charge e . A great merit of circular Rydberg atoms is that the lifetime of radiative decay is very long, scaling as n^5 with the principal quantum number n , and $\sim O[1 \text{ ms}]$ for $n \sim 25$ [11].

The wave function ψ_{nlm} of a circular Rydberg state of a principal quantum number n is given by

$$\psi_{n, n-1, \pm(n-1)}(\vec{r}) \propto e^{\pm i(n-1)\varphi} (r^2 - z^2)^{(n-1)/2} e^{-r/(n a_B)}, \quad (71)$$

with the magnetic quantum number $m = \pm(n - 1)$, and a_B is the Bohr radius. For large coordinate arguments $r \gg |z|$, Rydberg states in general have the radial wave function of the form

$$R_{n-1}(r) \propto r^{n-1} e^{-r/(na_B)}. \quad (72)$$

Momentum representation of Rydberg states is also useful, as shall be shown in the following. Appendix B describes momentum space representation of the wave function.

For subsequent discussion it will become important to compute a correlation integral of the initial and the final wave functions of the atomic electron,

$$a_{if}(\vec{\Delta}) = \int \frac{d^3x}{(2\pi)^3} e^{-i\vec{\Delta}\cdot\vec{x}} \psi_f^*(\vec{x}) \psi_i(\vec{x}), \quad (73)$$

where $\vec{\Delta} = \vec{q}_1 + \vec{q}_2$ is the sum of emitted neutrino momenta. We assume that both the initial and the final electron states have definite azimuthal angular momentum components, m_i , m_f along the microwave propagation, taken as the z -axis. Using the expansion formula

$$e^{-i\vec{\Delta}\cdot\vec{x}} = \sum_l i^l (2l+1) j_l(\Delta r) P_l(\cos\theta'), \quad (74)$$

$$\cos\theta' = \cos\theta_\Delta \cos\theta + \sin\theta_\Delta \sin\theta \cos(\varphi_\Delta - \varphi), \quad (75)$$

along with the addition theorem of the spherical harmonics

$$(2l+1)P_l(\cos\theta') = 4\pi \sum_m Y_{lm}^*(\theta_\Delta, \varphi_\Delta) Y_{lm}(\theta, \varphi), \quad (76)$$

one readily derives $m = m_f - m_i$ after the angular φ integration in Eq. (73).

For simplicity we shall work out the correlation integral only for the transition from a circular to a circular state. The result is

$$a_{if}(\vec{\Delta}) \approx \frac{i^{n_i-n_f}}{\pi\sqrt{2\pi}} c(n_i, n_f) \mathcal{P}_{n_i-n_f}^{n_f-n_i}(\cos\theta_\Delta) e^{i(n_f-n_i)\varphi_\Delta} \times \int_0^\infty dr r^2 j_{n_i-n_f}(\Delta r) R_{n_f n_f-1}(r) R_{n_i n_i-1}(r), \quad (77)$$

$$c(n_i, n_f) = \int_{-1}^1 d\cos\theta \mathcal{P}_{n_f-n_i}^{n_f-n_i}(\cos\theta) \times \mathcal{P}_{n_f-1}^{n_f-1}(\cos\theta) \mathcal{P}_{n_i-1}^{n_i-1}(\cos\theta), \quad (78)$$

where $\mathcal{P}_n^m(x)$ is the normalized, associated Legendre polynomial. We have taken the leading term in the l sum, $l = |n_i - n_f|$. In the large n limit of the principal quantum number,

$$c(n_i, n_f) \sim \pi^{-1/4} \left(\frac{n_i}{n_f}\right)^{1/4} \left(\frac{\Gamma((n_i - n_f + 3)/2)}{\Gamma((n_i - n_f + 2)/2)}\right)^{1/2}, \quad (79)$$

which is of order unity. The remaining radial integral is neither small for the region of

$$\Delta \leq \frac{2\sqrt{2}\pi}{a_B} \frac{1}{n^{3/2}}, \quad \delta n \sim \sqrt{\frac{n}{8}}, \quad (80)$$

with $\delta n = n_i - n_f \ll n_{i,f}$. For the transition around $n \approx$

20,

$$E_i - E_f \sim \frac{2\alpha^2 m_e \delta n}{n^3} \sim 11 \text{ meV} \left(\frac{20}{n}\right)^{5/2}, \quad (81)$$

$$\Delta \leq \Delta_{\max}, \quad \Delta_{\max} = 370 \text{ eV} \left(\frac{20}{n}\right)^{3/2}. \quad (82)$$

Thus, the correlation is large for a range of $\Delta \gg E_i - E_f$.

B. Field assisted pair decay

Suppose that the strong microwave is irradiated to a Rydberg state $|i\rangle$, which then decays into a neutrino pair + another Rydberg state $|f\rangle$;

$$R_i \rightarrow R_f + \nu_i \nu_j. \quad (83)$$

Electronic transition $|i\rangle \rightarrow |f\rangle$ under a strong electromagnetic (EM) field may be dealt with adopting quantum mechanical treatment of multiphoton processes [12], or its extension. One needs a theoretical formalism in order to properly incorporate strong field effects.

We consider a time-dependent EM field in the Hamiltonian taking the radiation gauge

$$H_1(t) = e \frac{\vec{A}(t) \cdot \vec{p}}{m_e} + e^2 \frac{\vec{A}^2(t)}{2m_e}. \quad (84)$$

The plane-wave microwave of a linear polarization is given by the vector potential of the form

$$\vec{A}(t) = \frac{\vec{E}_0}{\omega} \sin(\omega t), \quad (85)$$

while a circularly polarized case is

$$\vec{A}(t) = \frac{E_0}{\sqrt{2}\omega} (\sin(\omega t)\vec{e}_x \pm \cos(\omega t)\vec{e}_y), \quad (86)$$

where \vec{e}_i is the orthonormal unit vector along the i -axis. We took the z -axis as the direction of light propagation. In both cases of the polarization E_0 is the rms amplitude.

In discussions that follow it is important to distinguish whether the field is in the strong or the weak range of the strength. This may be characterized by interaction strength relative to its frequency;

$$\frac{eE_0 p}{m_e \omega^2} \sim 8 \times 10^3 n^{-1} \frac{E_0}{\text{V cm}^{-1}} \left(\frac{\text{GHz}}{\omega}\right)^2. \quad (87)$$

Depending on a combination of parameters, $E_0/(\omega^2 n)$, this can be either in the strong or the weak field range. Even if the field strength is strong in this sense, it may be arranged that the field is not large enough to ionize the Rydberg electron, $eE_0 < \alpha/(n^2 a_B)$ (attractive force from nucleus), which means

$$E_0 < 7 \times 10^{11} n^{-2} \text{V cm}^{-1}. \quad (88)$$

We would like to treat the weak interaction process alone perturbatively, and solve interaction of atomic electrons

with microwave as analytically as possible. As discussed in Appendix B, the transition amplitude of the neutrino pair emission is given by

$$(S-1)_{fi} \sim -i \int \frac{d^3 q_1 d^3 q_2}{(2\pi)^6} \int \frac{d^3 p_f d^3 p_i}{(2\pi)^3} \int_{-\infty}^{\infty} dt_1 \langle A_f(\infty) | \vec{p}_f \rangle \times \langle \vec{p}_f | U_A(\infty, t_1) H_W U_A(t_1, -\infty) | \vec{p}_i \rangle \times \langle \vec{p}_i | A_i(-\infty) \rangle. \quad (89)$$

Here H_W is the weak interaction Hamiltonian of the neutrino pair emission of momenta \vec{q}_i .

States taken as initial and final ones in Eq. (89), $U_A(t, -\infty) | A_i(-\infty) \rangle$ and $U_A(t, \infty) | A_i(\infty) \rangle$, are bound state solutions of the Schrödinger equation governed by the Hamiltonian of Coulomb potential plus the microwave field. Their momentum space representation $U_A(t, -\infty) | \vec{p}_i \rangle$ and $U_A(t, \infty) | \vec{p}_f \rangle$ are used here. The approximation, taken by Keldysh [13] and the one we shall also adopt, is to neglect the Coulomb interaction during the occurrence of the weak process, and use the plane-wave solution under the periodic field, known as the Volkov solution [12]; the time-dependent part in this approximation is

$$\langle \vec{p}_f | U_A(\infty, t) | \vec{p}_f \rangle \langle \vec{p}_i | U_A(t, -\infty) | \vec{p}_i \rangle \propto \exp \left[-i \left(\frac{\vec{p}_i^2 - \vec{p}_f^2}{2m_e} t + \frac{(\vec{p}_i - \vec{p}_f) \cdot \int_{-\infty}^t dt_1 \vec{A}(t_1)}{m_e} \right) \right],$$

neglecting irrelevant phase factors.

The Keldysh approximation is valid if the correction of the binding is small. This condition is worked out in [14], and in our case it leads to the frequency condition, as discussed in Appendix B,

$$\omega \leq 2.1 \times 10^6 n^{-4} \text{ GHz}, \quad (90)$$

with n the maximal principal quantum number during the transition. The field strength is also limited as in Appendix B.

The weak Hamiltonian H_W of the neutrino pair emission is translationally invariant, hence its matrix element contains the momentum conserving delta function;

$$\begin{aligned} & \langle \vec{p}_f | U_A(\infty, t) H_W U_A(t, -\infty) | \vec{p}_i \rangle \\ &= \exp \left[-i \left(\left(\frac{p_i^2}{2m_e} - \frac{p_f^2}{2m_e} - E_1 - E_2 \right) t + \frac{(\vec{p}_i - \vec{p}_f) \cdot \int_{-\infty}^t dt_1 \vec{A}(t_1)}{m_e} \right) \right] \frac{G_F}{\sqrt{2}} (2\pi)^3 \\ & \times \delta(\vec{p}_i - \vec{p}_f - \vec{q}_1 - \vec{q}_2) \sum_{ij} \langle f_\nu | j_{ij} | 0 \rangle \cdot \langle f | j_{ij}^e | i \rangle. \end{aligned} \quad (91)$$

The neutrino pair is not observed, hence one takes the helicity and momentum summation of neutrinos. The helicity summation of

$$\sum_{hh'} \sum_{ij} |\langle f_\nu | j_{ij} | 0 \rangle \cdot \langle f | j_{ij}^e | i \rangle|^2$$

has been examined in Sec. III in detail, yielding in the leading approximation of $1/m_e$, the matrix element squared of the form $(2 - m_1 m_2 / (E_1 E_2))$, Eq. (28), times the electron wave function factors.

To proceed further for computation of the transition amplitude squared, we insert a convenient identity,

$$\int d\vec{\Delta} \int dE_{12} \delta(\vec{\Delta} - \vec{q}_1 - \vec{q}_2) \delta(E_{12} - E_1 - E_2) = 1,$$

with $E_i = \sqrt{q_i^2 + m_i^2}$ neutrino momenta, and use

$$\begin{aligned} & \left| \int \frac{d^3 q_1 d^3 q_2}{(2\pi)^6} \int d\vec{\Delta} \int dE_{12} (2\pi)^3 \delta(\vec{\Delta} - \vec{q}_1 - \vec{q}_2) \right. \\ & \quad \times \delta(E_{12} - E_1 - E_2) f(\vec{q}_1, \vec{q}_2) \left. \right|^2 \\ &= \int d\vec{\Delta} \int dE_{12} \int \frac{d^3 q_1 d^3 q_2}{(2\pi)^3} \delta(\vec{\Delta} - \vec{q}_1 - \vec{q}_2) \\ & \quad \times \delta(E_{12} - E_1 - E_2) |f(\vec{q}_1, \vec{q}_2)|^2. \end{aligned} \quad (92)$$

Neutrino momentum integration here is

$$\begin{aligned} K_{ij}^M(E_{12}, \vec{\Delta}) &= \int \frac{d^3 q_1 d^3 q_2}{(2\pi)^3} \delta(\vec{\Delta} - \vec{q}_1 - \vec{q}_2) \\ & \quad \times \delta(E_{12} - E_1 - E_2) \left(2 - \frac{m_1 m_2}{E_1 E_2} \right) \end{aligned} \quad (93)$$

$$\begin{aligned} &= \frac{1}{(2\pi)^2} \sqrt{\left(1 - \frac{(m_1 + m_2)^2}{s_{12}} \right) \left(1 - \frac{(m_1 - m_2)^2}{s_{12}} \right)} \\ & \quad \times \left(E_{12}^2 \left(1 + \frac{m_1^2 - m_2^2}{s_{12}} \right) - \frac{E_{12}^2}{2} \left(1 + \frac{m_1^2 - m_2^2}{s_{12}} \right)^2 \right. \\ & \quad \left. - m_1 m_2 - \frac{\vec{\Delta}^2}{6} \left(1 - \frac{(m_1 + m_2)^2}{s_{12}} \right) \left(1 - \frac{(m_1 - m_2)^2}{s_{12}} \right) \right), \\ s_{12} &= E_{12}^2 - \vec{\Delta}^2. \end{aligned} \quad (94)$$

In the massless neutrino limit

$$K_{ij}^M(E_{12}, \vec{\Delta}) \rightarrow \frac{1}{8\pi^2} \left(E_{12}^2 - \frac{\vec{\Delta}^2}{3} \right). \quad (95)$$

The threshold behavior of this quantity at $s_{12} \rightarrow (m_1 + m_2)^2$ is

$$K_{ij}^M(E_{12}, \vec{\Delta}) \sim \frac{(m_1 m_2)^{3/2}}{2\pi^2 (m_1 + m_2)^2} \sqrt{E_{12}^2 - \vec{\Delta}^2 - (m_1 + m_2)^2}. \quad (96)$$

The transition probability is further simplified first by using

$$\begin{aligned} \langle \vec{p}_i | e^{-i\vec{p}_i^2 t / (2m_e)} | A_i(-\infty) \rangle &= \langle \vec{p}_i | e^{-iH_0 t} | A_i(-\infty) \rangle \\ &= e^{-iE_i t} \langle \vec{p}_i | A_i(-\infty) \rangle, \end{aligned} \quad (97)$$

and a similar relation for the final state, to replace the time-dependent factor to $e^{-i(E_i - E_f)t}$. When the Fourier transformation back to the configuration space is made, one obtains

$$\begin{aligned} \int \frac{d^3 p_f d^3 p_i}{(2\pi)^3} \delta(\vec{p}_i - \vec{p}_f - \vec{\Delta}) \langle A_f(\infty) | \vec{p}_f \rangle \langle \vec{p}_i | A_i(-\infty) \rangle \\ = \int \frac{d^3 x}{(2\pi)^3} e^{i\vec{\Delta} \cdot \vec{x}} \psi_f^*(\vec{x}) \psi_i(\vec{x}) \equiv a_{if}(\vec{\Delta}). \end{aligned} \quad (98)$$

The transition probability is then

$$\begin{aligned} |(S-1)_{fi}|^2 &= \frac{G_F^2}{2} \int d\vec{\Delta} |a_{if}(\vec{\Delta})|^2 \int_{\sqrt{\vec{\Delta}^2 + (m_1 + m_2)^2}}^{\infty} \\ &\times dE_{12} K_{ij}^M(E_{12}, \vec{\Delta}) \left| \int_{-\infty}^{\infty} dt \mathcal{F}_{if}(E_{12}, \vec{\Delta}; t) \right|^2, \end{aligned} \quad (99)$$

$$\mathcal{F}_{if}(E_{12}, \vec{\Delta}; t) = \exp \left[-i \left(\Delta_{if} t + \int_{-\infty}^t dt_1 \frac{e\vec{\Delta} \cdot \vec{A}(t_1)}{m_e} \right) \right], \quad (100)$$

$$\Delta_{if} = E_i - E_f - E_{12}. \quad (101)$$

In the formula (99) three important factors are separated: the integrated neutrino factor K_{ij}^M , the initial and the final electron factor $|a_{ij}(\vec{\Delta})|^2$, and the time dependence factor \mathcal{F}_{if} related to microwave irradiation. This essential simplification owes to the Keldysh approximation.

The time integral for this S -matrix element involves the time interval of infinite duration. In practice, it is important to understand a finite time integral of the form

$$\begin{aligned} \int_{t_0}^t dt_1 \mathcal{F}_{if}(E_{12}, \vec{\Delta}; t_1) &= \int_{t_0}^t dt_1 \exp \left[-i \left(\Delta_{if} t_1 + \int_{-\infty}^{t_1} dt_2 \right. \right. \\ &\times \left. \left. \frac{e\vec{\Delta} \cdot \vec{A}(t_2)}{m_e} \right) \right]. \end{aligned} \quad (102)$$

The analysis of this time-dependent phenomena is separated into two parts; in the first part we present the conventional multiphoton picture, which corresponds to the narrow band region of a more general analysis in the last subsection. There exists the additional wide band region which typically exhibits the exponentially growing instability, a phenomenon very time dependent. Only a lower limit of the growing rate is estimated in the wide band region. The real process goes with these two mechanisms entangled, hence it is complicated.

C. Multiphoton picture

We postpone a general analysis of Eq. (102), and concentrate here on an approximate expansion that leads to interpretation based on multiphoton processes. The multiphoton process has been described in many textbooks; for instance in [12] for the strong laser field, and in [1, 15] for microwave or rf fields.

We shall first discuss the case of linear microwave polarization. Using the expansion in terms of the Bessel function $J_N(x)$,

$$e^{-ib \sin \omega t} = \sum_{N=-\infty}^{\infty} J_N(b) e^{-iN\omega t}, \quad b = \frac{e\vec{\Delta} \cdot \vec{E}_0}{m_e \omega^2}. \quad (103)$$

Equation (102) becomes a sum of simple exponentials. The time integral is then readily computed, leading in the large time limit to

$$\int_{t_0}^t dt_1 \mathcal{F}_{if}(E_{12}, \vec{p}_i, \vec{p}_f; t_1) \rightarrow 2\pi \sum_N J_N(b) \delta(\Delta_{if} + N\omega). \quad (104)$$

The argument of the delta function implies the simple energy conservation, due to (101).

It would be instructive to numerically estimate the important quantity that appears in these formulas; the magnitude of microwave interaction,

$$b \sim \frac{eE_0 \Delta}{m_e \omega^2} \approx 0.2 \frac{\Delta}{0.1 \text{ eV}} \frac{E_0}{\text{V cm}^{-1}} \left(\frac{\text{GHz}}{\omega} \right)^2. \quad (105)$$

The momentum scale Δ has been set here to around 2 times the neutrino mass. This parameter b can be very large. The Bessel function $J_N(b)$ is maximal at $b \approx |N|$.

Using the standard formula

$$\lim_{t \rightarrow \infty} \frac{|2\pi \delta(\Delta)|^2}{t} = 2\pi \delta(\Delta),$$

we derive at a time-independent rate $w = \lim_{t \rightarrow \infty} P(t)/t$ of the form

$$\begin{aligned} w &= \sum_N w_N, \\ w_N &= \pi G_F^2 \int d\vec{\Delta} |a_{if}(\vec{\Delta})|^2 \left| J_N \left(\frac{e\vec{\Delta} \cdot \vec{E}_0}{m_e \omega^2} \right) \right|^2 \\ &\times \int_{\sqrt{\vec{\Delta}^2 + (m_1 + m_2)^2}}^{\infty} dE_{12} \\ &\times \delta(E_{12} - N\omega - E_i + E_f) K_{ij}^M(E_{12}, \vec{\Delta}). \end{aligned} \quad (106)$$

There is a minimum number of photons N_0 in the N summation; $N > N_0$ with

$$N_0 = \frac{1}{\omega} \left(\sqrt{\vec{\Delta}^2 + (m_1 + m_2)^2} - E_i + E_f \right). \quad (107)$$

This N_0 can be negative. A negative N_0 means that stimulated microwave photons are emitted (instead of absorbed)

to cause the neutrino pair emission. The requirement for a negative N_0 is

$$E_i - E_f > m_1 + m_2. \quad (108)$$

For the weak field the neutrino pair emission rate is in proportion to

$$\left| J_N \left(\frac{e\vec{\Delta} \cdot \vec{E}_0}{m_e \omega^2} \right) \right|^2 \propto \left(\frac{E_0}{\omega} \right)^{2|N|}. \quad (109)$$

Interpretation of this result is that there are contributions from N photon absorption for $N > 0$ or $-N$ emission for $N < 0$, which feed or take away energy $|N|\omega$ to cause the multiphoton transition. Roughly, the relation to the neutrino mass m_i , $m_1 + m_2 \approx E_i - E_f + N\omega$ holds. Suppose that the final state is specified. When $E_f > E_i$ (the case of upper level), only microwave absorption is possible for the pair emission. When $E_f < E_i$ (the case of lower level), both absorption and emission is possible according to the sign of $m_1 + m_2 - (E_i - E_f)$. Since the rate is maximal at $|N| \approx b \propto E_0$, the adjustment of the field amplitude E_0 can help to locate the position of the threshold of $E_i - E_f = m_1 + m_2$.

The neutrino pair emission accompanying $N(>0)$ microwave absorption occurs as if a hypothetical heavy ‘‘boson’’ of mass $N\omega + E_i - E_f$ decays according to the rate w_N . Let us clarify this process in the weak field limit. The neutrino pair emission caused by N multiphoton transition occurs with interaction strength,

$$\frac{G_F}{\sqrt{2}} \frac{1}{N!} \left(\frac{e\vec{\Delta} \cdot \vec{E}_0}{2m_e \omega} \right)^N. \quad (110)$$

This is the E1 transition repeated N times plus the weak pair emission. The hypothetical boson does not have a definite momentum to be transmitted to the neutrino pair, but the conservation law is replaced by

$$(2\pi)^3 \delta(\vec{\Delta}) \rightarrow |a_{if}(\vec{\Delta})|^2.$$

There is nothing special about this, because both initial and final states are not momentum eigenstates. The momentum distribution has a width $\approx \alpha^2 m_e / n^3$. The total rate is a sum over N of many multiphotons. A large mass ‘‘particle’’ of $N \gg 1$ might be called a heavy electron due to many photon clouds. The rate of a very heavy electron decay is suppressed by

$$\left(\frac{1}{N!} \right)^2 \left(\frac{E_i - E_f - E_{12}}{2\omega} \right)^{2N}, \quad (111)$$

because the Bessel function behaves as $|J_N(b)| \sim (b/2)^{2N}/(N!)^2$.

To obtain a large rate, it is necessary to have many contributions of different N . The property of the Bessel function $J_N(b)$ tells that the N sum can be large when N is of order b or less. The ratio b/N , in particular

$$\frac{b}{|N_0|} = \frac{e\vec{\Delta} \cdot \vec{E}_0}{\sqrt{\Delta^2 + (m_1 + m_2)^2} m_e \omega}, \quad (112)$$

can however be small, especially if $\Delta \gg m_1 + m_2$, because in this case

$$\frac{b}{|N_0|} = O \left[\frac{eE_0}{m_e \omega} \right] \sim O[0.9 \times 10^{-5}] \frac{E_0}{V \text{ cm}^{-1}} \frac{\text{GHz}}{\omega}. \quad (113)$$

Thus, it is important to have for N_0 a small, or better, a negative number such that the N sum contains contributions from small N 's.

A better, but still crude way of estimating a number of multiphoton contributions of many paths, hence the pair emission rate is as follows. Take \vec{E}_0 along the z direction. For a given Δ_z , there is a region of relatively large value of the Bessel function $J_N(b)$ at $b \approx N \gg 1$,

$$J_N \left(\frac{e\Delta_z E_0}{m_e \omega^2} \right) \sim c \left(\frac{m_e \omega^2}{e\Delta_z E_0} \right)^{1/3}, \quad c = \frac{\Gamma(1/3)}{2^{2/3} 3^{1/6} \pi} \sim 0.45. \quad (114)$$

Replacing the Bessel function by this gives the rate

$$w = \pi c^2 G_F^2 \int d\vec{\Delta} K_{ij}^M \left(\frac{e\Delta_z E_0}{m_e \omega} + E_i - E_f, \vec{\Delta} \right) \times |a_{if}(\vec{\Delta})|^2 \left(\frac{m_e \omega^2}{e\Delta_z E_0} \right)^{2/3}. \quad (115)$$

The threshold behavior of the rate based on (115) may be derived using the neutrino factor K_{ij}^M near the threshold, (96). For this estimate we assume the correlation integral of order unity $a_{ij} = O[1]$, to give

$$c^2 G_F^2 J \frac{(m_1 m_2)^{3/2}}{(m_1 + m_2)^2} \left(\frac{m_e \omega^2}{eE_0} \right)^{2/3} \sum_N ((N\omega + E_i - E_f)^2 - (m_1 + m_2)^2)^{5/3}, \quad (116)$$

where J is

$$J = \int_0^1 d\rho \rho (1 - \rho^2)^{5/6} \int_0^1 dz z^{-2/3} \sqrt{1 - z^2}, \quad c^2 J \sim 0.15. \quad (117)$$

The N summation is limited by

$$N < N_{\max}, \quad (118)$$

$$N_{\max} = O \left[\frac{eE_0 \Delta_{if}}{m_e \omega^2} \right] \sim 0.2 \frac{E_0}{V \text{ cm}^{-1}} \frac{m_\nu}{50 \text{ meV}} \left(\frac{\text{GHz}}{\omega} \right)^2,$$

where Δ_{if} is a typical momentum transfer of order $m_1 + m_2$.

The enhancement factor R may be defined relative to the standard rate near the threshold, $G_F^2 (m_1 + m_2)^5 / (15\pi^3)$;

$$R \sim \frac{45\pi^3 c^2 J}{16} \left(\frac{m_e \omega^2}{eE_0} \right)^{5/3} \frac{(m_1 m_2)^{3/2}}{\omega^2 \Delta_{if} (m_1 + m_2)^7} \\ \times \left(\left(\frac{eE_0 \Delta_{if}}{m_e \omega} + E_i - E_f \right)^2 - (m_1 + m_2)^2 \right)^{8/3}. \quad (119)$$

For the weak field of $eE_0/(m_e \omega) \ll 1$, the threshold appears at $E_f = E_i - m_1 - m_2$. It may also appear as a threshold of the field amplitude E_0 . A large power $8/3$ implies that the rate quickly increases once the threshold is passed.

Well above the threshold one may use Eq. (95), and the rate and the enhancement factor become of order

$$\frac{27c^2 G_F^5 \omega^5}{448} \left(\frac{m_e \omega}{eE_0} \right)^{2/3} \left(N_{\max} + \frac{E_i - E_f}{\omega} \right)^{16/3}, \quad (120)$$

$$R \sim 5.6 \left(\frac{eE_0}{m_e \omega} \right)^{14/3} \left(\frac{m_1 + m_2}{\omega} \right)^{1/3}, \quad (121)$$

taking $\Delta_{if} = m_1 + m_2$. This factor is very sensitive to the microwave power $\propto P^{7/3}$ and its frequency $\propto \omega^{-5}$, and its precise determination requires a more elaborate computation.

There is also contribution from the $N < b$ region of the Bessel function $J_N(b) \sim \sqrt{\frac{\pi}{2b}}$. This contribution is estimated as

$$w_{N < b} = O \left[\frac{\pi G_F^2 (\Delta E)^5}{240} \frac{m_e \omega}{eE_0} \right]. \quad (122)$$

We shall finally consider the case of circular polarization. In this case

$$\vec{\Delta} \cdot \vec{A}(t) = \frac{E_0 \Delta}{\sqrt{2} \omega^2} \sin \theta_\Delta \sin(\omega t \pm \varphi_\Delta), \quad (123)$$

$\theta_\Delta, \varphi_\Delta$ being angle factors of the momentum $\vec{\Delta}$. The expansion in terms of the Bessel function becomes

$$\exp \left[i e \frac{\vec{\Delta} \cdot \vec{A}(t)}{m_e} \right] = \sum_{N_d} J_{N_d} \left(\frac{e E_0 \Delta \sin \theta_\Delta}{\sqrt{2} m_e \omega^2} \right) \\ \times \exp[-i N_d \omega t \mp i N_d \varphi_\Delta]. \quad (124)$$

The pair emission rate for a circular to a circular transition is given in terms of the correlation integral by

$$w = 2\pi^2 G_F^2 \int_0^\infty d\Delta \Delta^2 \int_{-1}^1 d \cos \theta_\Delta |a_{if}(\Delta)|^2 \\ \times \mathcal{P}_{n_f+n_i-1}^{n_f-n_i}(\cos \theta_\Delta) \times \theta(E_i - E_f \mp (n_i - n_f)\omega) \\ - \sqrt{\Delta^2 + (m_1 + m_2)^2} \times \left| J_{n_i-n_f} \left(\frac{e E_0 \Delta \sin \theta_\Delta}{\sqrt{2} m_e \omega^2} \right) \right|^2 \\ \times K_{ij}^M(E_i \mp (n_i - n_f)\omega - E_f, \Delta). \quad (125)$$

A detailed and more precise rate computation in the multiphoton picture shall be presented elsewhere, and be compared to a more general approach presented in the

following subsection. The method described in the present subsection has a limitation, and is interpreted as a part of more general approach we shall now describe.

D. Relevance of parametric resonance

Consider the time-dependent part of the rate

$$\mathcal{W}_{if}(t; E_{12}, \vec{\Delta}) = \text{Re} \left(\mathcal{F}_{if}^*(t) \int_{t_0}^t dt_1 \mathcal{F}_{if}(t_1) \right), \quad (126)$$

which appears in the transition rate given by the time derivative of the transition probability (99), namely

$$w(t) = \frac{G_F^2}{2} \int d\vec{\Delta} |a_{if}(\vec{\Delta})|^2 \int_{\sqrt{\Delta^2 + (m_1 + m_2)^2}}^\infty dE_{12} K_{ij}^M(E_{12}, \vec{\Delta}) \\ \times \mathcal{W}_{if}(t; E_{12}, \vec{\Delta}). \quad (127)$$

We define a complex function $G(t; a, b)$ in terms of new dimensionless variables a, b

$$G(t; a, b) = e^{ia\omega t + ib \sin \omega t} \int_0^t dt' e^{-ia\omega t' - ib \sin \omega t'}, \quad (128)$$

$$a = \frac{E_i - E_f - E_{12}}{\omega}, \quad b = \frac{e \vec{\Delta} \cdot \vec{E}_0}{m_e \omega^2}, \quad (129)$$

such that $\mathcal{W}_{if}(t; E_{12}, \vec{\Delta}) = G(t; a(E_{12}), b(\vec{\Delta}))$.

The multiphoton picture in the preceding subsection corresponds to an infinite time limit ignoring a coherence in the computation of $G(t; a, b)$, which leads to a time-independent, constant rate $w(\infty)$. However, there exists an intrinsic instability in some parameter region of (a, b) , which we now discuss. A coherence effect at finite times is crucial in this discussion.

The quantity (129) satisfies a coupled differential equation,

$$\begin{pmatrix} \frac{d^2}{dt^2} + \omega^2(a + b \cos \omega t)^2 & -b\omega^2 \sin \omega t \\ b\omega^2 \sin \omega t & \frac{d^2}{dt^2} + \omega^2(a + b \cos \omega t)^2 \end{pmatrix} \\ \times \begin{pmatrix} \text{Re} G(t) \\ \text{Im} G(t) \end{pmatrix} = 0. \quad (130)$$

This system has an intrinsic frequency scale $|a|\omega = |E_i - E_f - E_{12}|$ such as given by the energy difference between the initial and the final states. This intrinsic scale is further modulated by a periodic variation of parameters whose frequency is ω and amplitude is $|b|$. Cooperative effects of external modulation with the intrinsic property gives rise to interesting phenomena of the parametric amplification.

In our time-dependent problem, the initial condition is specified as

$$G(0) = 0, \quad \dot{G}(0) = 1. \quad (131)$$

Thus, there is no way to avoid the instability of the para-

metric resonance, once the parameters (b, a) fall in the instability band.

General theory [16] of linear differential equations with periodic coefficients indicates solutions of the Mathieu type, and the unstable and stable band structure appears in the parameter (b, a) plane. In the unstable band the exponential growth is observed;

$$\text{Re}(e^{\Gamma(a,b)t/2 - i(E_i - E_f - E_{12})t} f(\omega t)), \quad (132)$$

with $f(\tau)$ a periodic function, hence the instability greatly expedites depletion of the prepared state. The parameter b is essentially \propto the total momentum of the neutrino pair Δ_z projected onto the microwave electric field direction taken the z -axis here, which is also a typical momentum transfer in the electron transition $|i\rangle \rightarrow |f\rangle$. Another one $a \propto E_{12} - E_i + E_f$ is the total neutrino energy minus the mass difference $E_i - E_f$. Thus, $(b, a) \propto (\Delta_z, E_{12} - E_i + E_f)$, and the unstable band structure in (b, a) plane signifies where in the phase space of the neutrino pair contributes to the emission rate. The instability signifies an exponential decay of the initially prepared state.

The relative weight of the b term in Eq. (130), the magnitude $|b|/|a|$, signifies the importance of the parametric amplification. Roughly, the narrow band region is in the parameter region of $|b| \ll |a|$, and the wide band region is in $|b| \gg |a|$. The multiphoton picture explained in the previous subsection corresponds to a narrow band of instability. The N th band in the narrow band region corresponds to a mass difference of initial and final states, $N\omega + E_i - E_f$ shifted by the energy input of N microwave photons. The narrowness implies weaker rates. The diagrammatic interpretation of the narrow band decay has been given in the literature [17]. The correspondence between the two regions is given by

$$\sum_N \left| J_N \left(\frac{e\vec{\Delta} \cdot \vec{E}_0}{m_e \omega^2} \right) \right|^2 2\pi \delta(N\omega + E_i - E_f - E_{12}) \leftrightarrow \mathcal{W}_{if}(t; E_{12}, \vec{\Delta}). \quad (133)$$

Rather than a discrete N sum of multiphotons there is a continuous spectrum of heavy electrons of mass E_{12} present in the wide band region.

The wide band region gives a much more enhanced time-dependent rate than the narrow band multiphoton result presented in the previous subsection [18]. If (b, a) lies deeper in the instability band, namely, the larger $|b|/|a|$ is, the greater the rate is. The rate readily exceeds order unity (in the unit of $1/\omega$, that is $\Gamma = O[\omega]$) deep in an instability band. In the wide band region there is no definite number of multiphotons N , and the continuum broad mass $E_i - E_f$ range all contribute to the instability. If one experimentally arranges that there is no radiatively decaying state as in the cavity QED, then this means that the neutrino pair emission is expedited; enhanced pair

emission. It is thus important to depict the structure of stability-instability bands in the (b, a) plane.

The phase space region in terms of $(E_{12}, \vec{\Delta})$ of the wide band region is estimated as follows. One can imagine that the most important region is restricted to $|a| \leq |b|$ due to an experience in the Mathieu equation. For large b 's, the coupled equation (130) approximately decouples, and the coefficient term of the form $\propto (1 - \cos 2\omega t)$ implies that the relevant (b, a) region is indeed deep in wide band regions. The exponential growth rate given by $e^{\lambda\omega t}/(\lambda\omega)$ is of order $\lambda \approx 0.15/2$, as shown in [19].

The two constraints on the wide band region $|a| \leq |b|$ and the mass restriction correspond to a region of $(E_{12}, \vec{\Delta})$,

$$(E_{12} - E_i + E_f)^2 \leq \left(\frac{eE_0}{m_e \omega} \right)^2 \Delta_z^2, \quad (134)$$

$$E_{12}^2 \geq \vec{\Delta}^2 + (m_1 + m_2)^2.$$

This gives a neutrino pair momentum integration of order

$$2 \int d\vec{\Delta} |a_{if}(\vec{\Delta})|^2 \int_{E_i - E_f - \epsilon|\Delta_z|}^{E_i - E_f + \epsilon|\Delta_z|} dE_{12} K_{ij}^M(E_{12}, \vec{\Delta}) \times \mathcal{W}_{if}(t; E_{12}, \vec{\Delta}), \quad (135)$$

for $\epsilon \ll 1$ with

$$\epsilon = \left| \frac{eE_0}{m_e \omega} \right|. \quad (136)$$

For a stronger field, the phase space area is quite different. In particular, towards and above the critical strength E_c ,

$$E_c = \frac{m_e \omega}{e} \sim 1.1 \times 10^5 \text{ V cm}^{-1} \frac{\omega}{\text{GHz}}, \quad (137)$$

the momentum space integration is changed to

$$2 \int d\vec{\Delta} |a_{if}(\vec{\Delta})|^2 \left(\theta(\Delta_* - \Delta_z) \int_{E_i - E_f - \epsilon|\Delta_z|}^{E_i - E_f + \epsilon|\Delta_z|} dE_{12} + \theta(\Delta_z - \Delta_*) \int_{\sqrt{\Delta^2 + (m_1 + m_2)^2}}^{E_i - E_f + \epsilon|\Delta_z|} dE_{12} \right) \times K_{ij}^M(E_{12}, \vec{\Delta}) \mathcal{W}_{if}(t; E_{12}, \vec{\Delta}). \quad (138)$$

In the $\epsilon \gg 1$ limit the second term is dominant, and

$$\Delta_* \approx \frac{1}{\epsilon} (E_i - E_f + \sqrt{\Delta_x^2 + \Delta_y^2 + (m_1 + m_2)^2}).$$

We shall make a crude estimate for the pair emission rate in the wide band region by making two assumptions. We first introduce an average rate factor $\langle \mathcal{W}_{if} \rangle$, and next compute the rate far away from the threshold region for which one may use Eq. (95). The E_{12} integration then gives

$$\approx \int d\vec{\Delta} |a_{if}(\vec{\Delta})|^2 \frac{\epsilon^3}{24\pi^2} |\Delta_z|^3 \langle \mathcal{W}_{if} \rangle. \quad (139)$$

It is thus expected to obtain the rate larger than

$$w \approx \frac{G_F^2 \Delta_{\max}^6}{240\pi} \left(\frac{eE_0}{m_e \omega} \right)^3 \langle \mathcal{W}_{if} \rangle \quad (140)$$

$$\sim 6 \times 10^{-28} \text{ s}^{-1} (\langle \mathcal{W}_{if} \rangle \omega / 10) \left(\frac{E_0}{kV \text{ cm}^{-1}} \right)^3 \left(\frac{\text{GHz}}{\omega} \right)^4 \times \left(\frac{\Delta_{\max}}{400 \text{ eV}} \right)^6, \quad (141)$$

using Δ_{\max} of order, Eq. (82).

Once the large rate is confirmed, one may go to the threshold region, in which one replaces the energy integral by

$$\int_{\sqrt{\Delta^2 + (m_1 + m_2)^2}}^{E_i - E_f + \epsilon |\Delta_z|} dE_{12} K_{ij}^M(E_{12}, \vec{\Delta}) \sim \frac{(m_1 m_2)^{3/2}}{4\pi^2 (m_1 + m_2)^2} (E_i - E_f + \epsilon |\Delta_z|) \times \sqrt{(E_i - E_f + \epsilon |\Delta_z|)^2 - \vec{\Delta}^2 - (m_1 + m_2)^2}. \quad (142)$$

This gives the threshold rate, with $\epsilon = eE_0/(m_e \omega)$,

$$\frac{G_F^2 \Delta_{\max}^2}{6\pi} \frac{(m_1 m_2)^{3/2}}{(m_1 + m_2)^2 \epsilon^2} ((\epsilon \Delta_{\max} + E_i - E_f)^2 - (m_1 + m_2)^2)^{5/2} (\langle \mathcal{W}_{if} \rangle \omega / 10). \quad (143)$$

Above a field threshold of ($m_1 + m_2 = 2m_\nu$)

$$\frac{2m_e \omega m_\nu}{e \Delta_{\max}} \sim 3V \text{ cm}^{-1} \frac{m_\nu}{50 \text{ meV}} \frac{\omega}{\text{GHz}} \frac{400 \text{ eV}}{\Delta_{\max}}, \quad (144)$$

the rate quickly rises to a rate of order

$$w \approx \frac{G_F^2 \Delta_{\max}^5 m_\nu}{240\pi} \left(\frac{eE_0}{m_e \omega} \right)^3 \langle \mathcal{W}_{if} \rangle, \quad (145)$$

taking $m_i = m_\nu$. This rate is m_ν/Δ_{\max} times the rate much above the threshold.

A large factor by $(\Delta_{\max}/m_\nu)^5$ in these rates is due to a larger momentum spread in sharply localized circular Rydberg states.

The critical field strength for the circular polarization is a factor $\sqrt{2}$ larger, but the phase space is also different.

It is important to keep in mind that the coherence should be maintained during the microwave irradiation. If this is possible for a long time, one may expect a huge growth factor $\langle \mathcal{W}_{if} \rangle$. The ultimate bound on $\langle \mathcal{W}_{if} \rangle$ is derived by the unitarity argument in the following way [20]. The unitarity for the time-dependent process requires

$$\sum_f \int_{-\infty}^T dt' w_{fi}(t') \leq 1. \quad (146)$$

With a given time-dependent rate $w_{fi}(t)$, this is essentially a bound on the allowed time T . It is appropriate to parametrize our weak process with

$$w_{fi}(t) = A \left(\left(\frac{n_i}{n_f} \right)^2 - 1 \right)^5 e^{\lambda \omega t}, \quad (147)$$

due to the energy dependence of the weak transition $n_i \rightarrow n_f$ by the neutrino pair emission. The most important dependence is on the final state n_f , as indicated. We ignored less important dependence of λ, A on n_f . The requirement of the unitarity Eq. (146) is then roughly

$$\frac{A}{\lambda \omega} e^{\lambda \omega T} \int_{n_0}^{n_f} dn_f 4n_f \left(\left(\frac{n_i}{n_f} \right)^2 - 1 \right)^5 \leq 1. \quad (148)$$

For an estimate of n_0 we take the allowed lowest state for the pair emission, $E_i - E_f > 2m_\nu$,

$$\frac{\alpha^2 m_e}{2n_0^2} < 2m_\nu. \quad (149)$$

Taking as an order of magnitude estimate $n_0 = \sqrt{\alpha^2 m_e / (4m_\nu)}$ gives

$$\frac{A}{\lambda \omega} e^{\lambda \omega T} \leq \frac{5n_0^{10}}{2n_i^{12}} \sim 3 \times 10^{15} \left(\frac{20}{n_i} \right)^{12} \left(\frac{50 \text{ meV}}{m_\nu} \right)^5, \quad (150)$$

corresponding to the maximal rate

$$A e^{\lambda T} \left(\left(\frac{n_i}{n_f} \right)^2 - 1 \right)^5 \leq 3 \times 10^5 \text{ s}^{-1} \frac{\omega}{\text{GHz}} \left(\frac{50 \text{ meV}}{m_\nu} \right)^5 \times \left(\left(\frac{n_i}{n_f} \right)^2 - 1 \right)^5, \quad (151)$$

with $\lambda = 10$.

The actual rate would be very large, much larger than the number given in Eq. (141), but presumably less than the unitarity bound (151). A practical rate might be limited by actual experimental conditions such as the loss rate of coherence of Rydberg atoms. Most relaxation time may be arranged to be much larger than $10/\omega \approx 10^{-8} \text{ s} (\text{GHz}/\omega)$ such that the real rate may be close to the unitarity bound. There appears a real possibility of measuring the neutrino pair emission process from circular Rydberg states if the background rejection is successful.

It is beyond the scope of our present work to precisely locate and further exploit the wide band regions for the parametric amplification of the neutrino pair emission. A detailed study of this aspect will appear elsewhere.

VI. A FEW COMMENTS ON EXPERIMENTAL METHOD

Clearly, one needs a systematic study, both theoretical and experimental, to implement our idea of the neutrino pair emission from circular Rydberg atoms. We shall be content here to make a few, rather trivial, comments towards a more organized study.

Laser irradiated pair emission process is relatively straightforward, hence we shall focus on the microwave irradiated Rydberg atoms.

A. Key ideas for experimental success

One has to avoid the danger of disappearance of the initial Rydberg states via ordinary radiative decay, since it might also be enhanced by the wide band parametric resonance. For this purpose, we may use circular Rydberg states as the initial prepared state, for which radiative decays are very much suppressed except $n \rightarrow n-1$ E1 transition. This E1 transition can be suppressed for instance by the cavity QED effect [2]; radiative decay mode within a cavity is modified by the boundary effect, and if the wavelength $\lambda > 2d$, a size of the cavity, the decay may be inhibited. The inhibition prevails for all multiphoton transitions, since all photons in this case satisfy the same condition $\lambda > 2d$ once one photon transition is inhibited. One must however arrange experimental apparatus such that the cavity does not interfere with the microwave irradiation [21].

Another important issue is how to unambiguously identify the pair emission process. Identification of final states is most important for the determination of the threshold, and this can be done by the field ionization technique [1]. The threshold for the neutrino pair $\nu_i \nu_j$ appears at

$$\epsilon \Delta_{if} + E_i - E_f = m_i + m_j, \quad (152)$$

with $\epsilon = eE_0/(m_e \omega)$.

The best way for unambiguous identification of the weak process is to measure parity violating (PV) effects which are absent in QED processes. The simplest of this kind is to use a circularly polarized photon beam and to measure the difference of the atomic transition rate between $h = \pm 1$ polarization. The asymmetry of the emitted photon distribution along the direction of the polarization $\propto \vec{J} \cdot \vec{p}_\gamma$ is another parity violating measurable. A detailed theoretical study of this effect will appear elsewhere.

B. How to proceed

Since the small rate is a critical issue, an organized strategy of experimental efforts is important. We believe that the first step should be the discovery of the neutrino pair emission from excited atoms, and then one should steadily approach the smaller energy scale towards the pair emission threshold. Presumably, at a few times twice the heaviest neutrino mass of order 0.05 eV, namely, at energy ≈ 0.3 eV, one can hope to observe a signature of the difference between the Majorana and the Dirac neutrino. The final step is a precision neutrino mass spectroscopy along with the measurement of mixing angles.

The use of atoms for neutrino physics is a new concept. It is evident that many R and D are required for this project, but one can initiate both experimental and theoretical efforts by use of modest human and budgetary resources. This is perhaps the ideal way towards a difficult physics goal.

ACKNOWLEDGMENTS

I would like to thank A. Fukumi, I. Nakano, H. Nanjo, and N. Sasao for many stimulating discussions, in particular, on experimental feasibility of the ideas presented here. N. Sasao has also pointed out a few mistakes in the original version of this manuscript, which is much appreciated. I also appreciate Y. Okabayashi for providing Fig. 2 in the revised version of this paper. This work was supported in part by the Grant-in-Aid for Science Research from the Ministry of Education, Science and Culture of Japan No. 13135207.

Note added.—After submission of this paper for publication, we realized that laser irradiated pair emission at lower thresholds $2m_1$ and $m_1 + m_2$ is useful for detection of the relic cosmic neutrino of 1.9K via the Pauli blocking effect. See [24] for this observation.

Note added in proof.—After submission of this paper for publication, an analysis based on the optical Bloch equation has been performed, and the greatest enhancement factor has been obtained, when the second laser is irradiated to the $|I^*\rangle \leftrightarrow |I^{**}\rangle$ transition. This work will be published elsewhere.

APPENDIX A: BASIC FORMULAS OF MAJORANA FIELD

Using the representation of the Clifford algebra

$$\gamma_\alpha \gamma_\beta + \gamma_\beta \gamma_\alpha = 2g_{\alpha\beta}, \quad (A1)$$

for γ_α (greek $\alpha = 0, 1, 2, 3$ and roman $i = 1, 2, 3$),

$$\gamma_0 = \begin{pmatrix} 0 & 1 \\ 1 & 0 \end{pmatrix}, \quad \gamma_i = \begin{pmatrix} 0 & \sigma_i \\ -\sigma_i & 0 \end{pmatrix}, \quad (A2)$$

$$\gamma_0 \gamma_i = \begin{pmatrix} -\sigma_i & 0 \\ 0 & \sigma_i \end{pmatrix}, \quad (A3)$$

$$\gamma_5 = i\gamma_0 \gamma_1 \gamma_2 \gamma_3 = \begin{pmatrix} -1 & 0 \\ 0 & 1 \end{pmatrix},$$

$$\psi = \begin{pmatrix} \varphi \\ \chi \end{pmatrix}, \quad \begin{pmatrix} \varphi \\ 0 \end{pmatrix} = \frac{1}{2}(1 - \gamma_5)\psi, \quad (A4)$$

$$\begin{pmatrix} 0 \\ \chi \end{pmatrix} = \frac{1}{2}(1 + \gamma_5)\psi,$$

the Dirac equation

$$i\gamma_\alpha \partial^\alpha \psi - m\psi = 0, \quad (A5)$$

is written in the following 2-component form:

$$(i\partial_t - i\vec{\sigma} \cdot \vec{\nabla})\varphi = m\chi, \quad (i\partial_t + i\vec{\sigma} \cdot \vec{\nabla})\chi = m\varphi. \quad (A6)$$

The identification, $\chi = i\sigma_2 \varphi^*$, in the Dirac equation gives the Majorana equation:

$$(i\partial_t - i\vec{\sigma} \cdot \vec{\nabla})\varphi = im\sigma_2 \varphi^*, \quad (A7)$$

with m the neutrino mass. The 2-component spinor φ belongs to $(1/2, 0)$ of the irreducible representation of the Lorentz group, while $i\sigma_2\varphi^*$ belongs to $(0, 1/2)$.

An explicit solution of helicity eigenstate is derived by solving the helicity eigen-equation of eigenvalue $h = \pm 1$,

$$\left(\frac{\vec{\sigma} \cdot \vec{p}}{p} - h\right) \begin{pmatrix} a \\ b \end{pmatrix} = 0, \quad \begin{pmatrix} a \\ b \end{pmatrix} = N \begin{pmatrix} p + hp_3 \\ h(p_1 + ip_2) \end{pmatrix}. \quad (\text{A8})$$

The full plane-wave solution to the Majorana equation is then

$$\varphi(x) = e^{-ip \cdot x} N \xi - e^{ip \cdot x} \frac{E_p + hp}{m} N^* i\sigma_2 \xi^*, \quad (\text{A9})$$

$$\xi = \xi(\vec{p}, h) = \begin{pmatrix} p + hp_3 \\ h(p_1 + ip_2) \end{pmatrix}. \quad (\text{A10})$$

An equivalent form of the solution is obtained by using

$$\frac{E_p + hp}{m} = \frac{\sqrt{E_p + hp}}{\sqrt{E_p - hp}}.$$

When the helicity operator $-i\vec{\sigma} \cdot \vec{\nabla}/|\vec{\nabla}|$ is applied, the first term gives the multiplicative factor h , while the second gives the factor $-h$. Thus, the consistent quantum interpretation of particle annihilation and antiparticle creation of two terms is given by Eq. (6).

The free quantum Majorana field is described by the Lagrangian density [3] of

$$\begin{aligned} \mathcal{L}_M = & \frac{1}{2}((\varphi^\dagger i\partial_0\varphi + \varphi^\dagger i\vec{\sigma} \cdot \vec{\nabla}\varphi) + (\text{H.c.})) \\ & - im(\varphi^\dagger \sigma_2 \varphi^* - \varphi^T \sigma_2 \varphi). \end{aligned} \quad (\text{A11})$$

The Majorana particle must be quantized according to the anticommutation rule

$$\{\varphi_\alpha(\vec{x}, t), \varphi_\beta^\dagger(\vec{y}, t)\}_+ = \delta^3(\vec{x} - \vec{y})\delta_{\alpha\beta}. \quad (\text{A12})$$

Mode decomposition in terms of plane waves is given by

$$\begin{aligned} \varphi(x) = & \sum_{\vec{p}, h} \left[c(\vec{p}, h) u(\vec{p}, h) e^{-ip \cdot x} + c^\dagger(\vec{p}, -h) \right. \\ & \left. \times \sqrt{\frac{E_p + hp}{E_p - hp}} (-i\sigma_2) u^*(\vec{p}, h) e^{ip \cdot x} \right], \end{aligned} \quad (\text{A13})$$

where

$$\{c(\vec{p}, h), c^\dagger(\vec{p}', h')\}_+ = \delta_{\vec{p}, \vec{p}'} \delta_{hh'}, \quad (\text{A14})$$

$$\{c(\vec{p}, h), c(\vec{p}', h')\}_+ = 0. \quad (\text{A15})$$

The relation of discrete and continuous momenta is given by

$$\delta_{\vec{p}, \vec{p}'} = \frac{(2\pi)^3}{V} \delta^{(3)}(\vec{p} - \vec{p}'), \quad \sum_{\vec{p}} f_{\vec{p}} = V \int \frac{d^3 p}{(2\pi)^3} f(\vec{p}), \quad (\text{A16})$$

with V the volume of the normalization box.

The normalization of the 2-spinor consistent with canonical anticommutation equation (A12) is derived as follows. Computing the anticommutator with the plane-wave mode decomposition gives

$$\begin{aligned} \{\varphi_\alpha(\vec{x}, t), \varphi_\beta^\dagger(\vec{y}, t)\}_+ = & \sum_{\vec{p}, h} \left[e^{i\vec{p} \cdot (\vec{x} - \vec{y})} |N(\vec{p}, h)|^2 (p + hp_3) \right. \\ & \times (p + h\vec{\sigma} \cdot \vec{p})_{\alpha\beta} + e^{-i\vec{p} \cdot (\vec{x} - \vec{y})} \\ & \times \frac{E_p + hp}{E_p - hp} |N(\vec{p}, h)|^2 \\ & \left. \times (p + hp_3)(p - h\vec{\sigma} \cdot \vec{p})_{\alpha\beta} \right]. \end{aligned} \quad (\text{A17})$$

We have used the relation

$$\xi(\vec{p}, h)\xi^\dagger(\vec{p}, h) = (p + hp_3)(p + h\vec{\sigma} \cdot \vec{p}). \quad (\text{A18})$$

The correct anticommutation relation thus requires

$$N(\vec{p}, h) = \frac{1}{2} \sqrt{\frac{E_p - hp}{pE_p(p + hp_3)}}. \quad (\text{A19})$$

Useful relations on the normalized wave function,

$$u(\vec{p}, h) = \frac{1}{2} \sqrt{\frac{E_p - hp}{pE_p(p + hp_3)}} \begin{pmatrix} p + hp_3 \\ h(p_1 + ip_2) \end{pmatrix}, \quad (\text{A20})$$

are

$$u(\vec{p}, h)u^\dagger(\vec{p}, h) = \frac{1}{4} \left(1 - \frac{hp}{E_p}\right) \left(1 + h\frac{\vec{\sigma} \cdot \vec{p}}{p}\right), \quad (\text{A21})$$

$$u^\dagger(\vec{p}, h)u(\vec{p}, h) = \frac{1}{2} \left(1 - \frac{hp}{E_p}\right). \quad (\text{A22})$$

In quantum field theory it is important to identify the Hamiltonian, momentum, and propagator. They are given for the Majorana field,

$$\begin{aligned} \mathcal{H}(\vec{x}) = & -i\varphi^\dagger \vec{\sigma} \cdot \vec{\nabla}\varphi + (\text{H.c.}) \\ & + \frac{im}{2} (\varphi^\dagger \sigma_2 \varphi^* - \varphi^T \sigma_2 \varphi), \end{aligned} \quad (\text{A23})$$

$$H = \int d^3x \mathcal{H}(\vec{x}) = \sum_{\vec{p}, h} E_p c^\dagger(\vec{p}, h) c(\vec{p}, h), \quad (\text{A24})$$

$$P = \int d^3x \varphi^\dagger(\vec{x}) (-i\vec{\nabla}) \varphi(\vec{x}) = \sum_{\vec{p}, h} \vec{p} c^\dagger(\vec{p}, h) c(\vec{p}, h), \quad (\text{A25})$$

$$\langle 0|T(\varphi(y)\varphi^\dagger(x))|0\rangle = -\sigma \cdot \partial \int \frac{d^4 p}{(2\pi)^4} \frac{e^{ip \cdot (y-x)}}{p^2 - m^2 + i\epsilon}, \quad (\text{A26})$$

$$\langle 0|T(\varphi(y)\varphi(x))|0\rangle = im\sigma_2 \int \frac{d^4 p}{(2\pi)^4} \frac{e^{ip \cdot (y-x)}}{p^2 - m^2 + i\epsilon}. \quad (\text{A27})$$

The energy (A24) and the momentum (A25) formulas of the Majorana field establish the correctness of identification of $c^\dagger(\vec{p}, h)$ and $c(\vec{p}, h)$ as particle creation and annihilation operators. The second form of the propagator (A27) is characteristic of the Majorana field that does not conserve the fermion number, and does vanish for the Dirac field.

APPENDIX B: WEAK PERTURBATIVE PROCESS FOR RYDBERG ATOMS UNDER MICROWAVE IRRADIATION

Consider a Hamiltonian system H_0 perturbed by 2 types of a generally time-dependent interaction, one of which with $H_0 + V_A(t)$ is treated as solvable, and V_B as very weak:

$$H = H_0 + V_A(t) + V_B, \quad H_0 = \frac{\vec{p}^2}{2m} + V_C(\vec{x}), \quad (\text{B1})$$

$$(i\partial_t - H_0 - V_A(t))|A_n(t)\rangle = 0, \quad (\text{B2})$$

$$|A_n(t)\rangle = U_A(t, t_0)|A_n(t_0)\rangle, \quad (\text{B3})$$

$$U_A(t, t_0) = \exp\left[-i \int_{t_0}^t dt_1 (H_0 + V_A(t_1))\right], \quad (\text{B3})$$

$$\langle A_n(t)| = \langle A_n(t_0)|U_A(t_0, t) = \langle A_n(t'_0)|U_A(t'_0, t). \quad (\text{B4})$$

In the interaction picture, the weak vertex is

$$V_B(t) = U_A^{-1}(t, t_0)V_B U_A(t, t_0). \quad (\text{B5})$$

The transition S matrix S is computed using solutions $|A_n(t)\rangle$ of (B2), from

$$\begin{aligned} \langle A_f(t_0)|V_B(t_1)|A_i(t_0)\rangle \\ = \langle A_f(t'_0)|U_A^{-1}(t_1, t'_0)V_B U_A(t_1, t_0)|A_i(t_0)\rangle. \end{aligned} \quad (\text{B6})$$

By taking the time limit of $t'_0 \rightarrow \infty$ and $t_0 \rightarrow -\infty$, the transition matrix element is to lowest order of V_B ,

$$\begin{aligned} (S - 1)_{fi} \sim -i \int_{-\infty}^{\infty} dt_1 \\ \times \langle A_f(\infty)|U_A^{-1}(t_1, \infty)V_B U_A(t_1, -\infty)|A_i(-\infty)\rangle. \end{aligned} \quad (\text{B7})$$

Expand states at time $= \pm\infty$ in terms of a complete set of momentum eigenstates;

$$|A_n(-\infty)\rangle = \int \frac{d^3 p |\vec{p}\rangle \langle \vec{p}| A_n(-\infty)\rangle}{(2\pi)^{3/2}}, \quad (\text{B8})$$

$$\begin{aligned} (S - 1)_{fi} \sim -i \int_{-\infty}^{\infty} dt_1 \int \frac{d^3 p_f \langle A_f(\infty)|\vec{p}_f\rangle \langle \vec{p}_f|}{(2\pi)^{3/2}} \\ \times U_A(\infty, t_1)V_B U_A(t_1, -\infty) \\ \times \int \frac{d^3 p_i |\vec{p}_i\rangle \langle \vec{p}_i| A_i(-\infty)\rangle}{(2\pi)^{3/2}}. \end{aligned} \quad (\text{B9})$$

We shall need to compute the transition matrix element for momentum eigenstates

$$\langle \vec{p}_f|U_A(\infty, t_1)V_B U_A(t_1, -\infty)|\vec{p}_i\rangle, \quad (\text{B10})$$

sandwiched between momentum state wave functions of

$$\langle A_f(\infty)|\vec{p}_f\rangle, \quad \langle \vec{p}_i|A_i(-\infty)\rangle. \quad (\text{B11})$$

States here

$$U_A(t, -\infty)|\vec{p}_i\rangle, \quad (\vec{p}_f|U_A(\infty, t))^\dagger = U_A(t, \infty)|\vec{p}_f\rangle, \quad (\text{B12})$$

are solutions of the Schrödinger equation, Eq. (B2).

These momentum state wave functions for the H atom are given in [22]. For instance, those of circular states of $l = |m| = n - 1$ are

$$\psi_{nn-1m}(\vec{p}) \propto e^{im\varphi} (1 - \cos^2\theta)^{(n-1)/2} \frac{(np)^{n-1}}{((np)^2 + p_0^2)^{n+1}}, \quad (\text{B13})$$

with $m = \pm(n - 1)$. For general states, using the atomic unit of $p_0 = 1/a_B$

$$\psi_{nlm}(\vec{p}) = F_{nl}(p)Y_{lm}(\theta, \varphi), \quad (\text{B14})$$

$$F_{nl}(p) \propto \frac{(np)^l}{((np)^2 + 1)^{l+2}} C_{n-l-1}^{l+1} \left(\frac{n^2 p^2 - 1}{n^2 p^2 + 1} \right), \quad (\text{B15})$$

where $C_N^x(x)$ is the Gegenbauer polynomial (of order N).

Both states, $U_A(t, -\infty)|A_i(-\infty)\rangle$ and $U_A(\infty, t)|A_f(\infty)\rangle$, contain the Coulomb and microwave field effects. Keldysh [13] neglects the Coulomb interaction. According to Reiss [14], this is justified if

$$r = \frac{\omega^2 a_B}{m_e} \times \frac{E^2}{\omega^4} \quad (\text{B16})$$

is small. ($\frac{E^2}{\omega^4}$ is the number of modes in the field.) This reduces to

$$r \leq \frac{E_c^2}{\alpha \omega^2 m_e^2} \quad (\text{B17})$$

in our problem. E_c is the maximum field allowed below ionization, given by

$$eE_c = \frac{\alpha}{(n^2 a_B)^2}. \quad (\text{B18})$$

Thus, the above parameter

$$r \leq \left(\alpha^2 \frac{m_e}{\omega} \right)^2 \frac{1}{n^8} \sim 4.3 \times 10^5 \left(\frac{\text{GHz}}{\omega} \right)^2 \left(\frac{10}{n} \right)^8. \quad (\text{B19})$$

This parameter is small if

$$\omega \leq 2.1 \times 10^6 \text{ GHz} n^{-4}, \quad (\text{B20})$$

and

$$E \leq E_C = \alpha^{5/2} m_e^2 n^{-4} \sim 5.2 \times 10^9 \text{ V cm}^{-1}. \quad (\text{B21})$$

Thus, we arrive at

$$U_A(t, -\infty)|\vec{p}\rangle \sim \exp \left[-i \int_{-\infty}^t dt_1 \left(\frac{\vec{p}^2}{2m} + \frac{\vec{p} \cdot \vec{A}(t_1)}{m} + \frac{e^2 \vec{A}^2(t_1)}{2m} \right) \right] |\vec{p}\rangle, \quad (\text{B22})$$

which is the Volkov solution [12], the exact plane-wave solution under a periodic field. Using an explicit form of $\vec{A}(t)$,

$$\int_{t_0}^t dt_1 \vec{A}(t_1) = \frac{\vec{E}_0}{\omega} \sin(\omega t) + (\text{const}). \quad (\text{B23})$$

Using the Volkov state (neglecting irrelevant constants), the matrix element is

$$\begin{aligned} & \langle \vec{p}_f | U_A(\infty, t) V_B U_A(t, -\infty) | \vec{p}_i \rangle \\ & \sim \exp \left[-i \left(\frac{\vec{p}_i^2 - \vec{p}_f^2}{2m} t + \frac{(\vec{p}_i - \vec{p}_f) \cdot \vec{E}_0}{m \omega^2} \sin(\omega t) \right) \right] \\ & \times \langle \vec{p}_f | V_B | \vec{p}_i \rangle. \end{aligned} \quad (\text{B24})$$

Time dependence of the relevant matrix element of the integrand of (B9)

$$\langle A_f(\infty) | \vec{p}_f \rangle \langle \vec{p}_f | U_A(\infty, t) V_B U_A(t, -\infty) | \vec{p}_i \rangle \langle \vec{p}_i | A_i(-\infty) \rangle, \quad (\text{B25})$$

is in Eq. (B24).

The high frequency Floquet theory (HFFT) of [23] that predicts dressed Coulomb potential caused by averaged field irradiation appears irrelevant in our parameter range of field strength and frequency.

-
- [1] T.F. Gallagher, *Rydberg Atoms* (Cambridge University Press, Cambridge, England, 1994).
- [2] R. G. Hulet, E. S. Hilfer, and D. Kleppner, Phys. Rev. Lett. **55**, 2137 (1985).
- [3] For a brief description of the Majorana field, see I. J. R. Aitchinson and A. J. G. Hey, *Gauge Theories in Particle Physics*, Vol II, Appendix P (IOP Publishing, London, 2004), p. 418.
- [4] We follow the notation of A. Cervera *et al.*, Nucl. Phys. **B579**, 17 (2000).
- [5] J. F. Nieves and P. B. Pal, Phys. Rev. D **32**, 1849 (1985), and references therein. They studied effect of Majorana masses in the pion energy spectrum for $K \rightarrow \pi + \nu\nu$. The result is discouraging due to a large mass of the kaon. The author would like to thank H. Nanjo and N. Sasao who raised a question on an identical particle effect of Majorana fermions.
- [6] M. Doi, T. Kotani, and H. Nishiura, Prog. Theor. Phys. **114**, 845 (2005), and references therein. This paper discusses the effect of Majorana neutrino combined with $V + A$ current in the muon decay. Without $V + A$ current the effect of Majorana neutrino is very small. The author should like to thank I. Nakano for bringing this work to his attention.
- [7] A preliminary idea of laser irradiated processes has been developed in collaboration with A. Fukumi, H. Nanjo, I. Nakano, and N. Sasao.
- [8] The author would like to thank A. Fukumi for preparing Fig. 1.
- [9] Y. Okabayashi (work in progress).
- [10] R. G. Hulet and D. Kleppner, Phys. Rev. Lett. **51**, 1430 (1983).
- [11] U. D. Jentschura *et al.*, J. Phys. B **38**, S97 (2005) and references therein.
- [12] B. H. Bransden and C. J. Joachain, *Physics of Atoms and Molecules* (Prentice-Hall, Englewood Cliffs, NJ, 2003), 2nd ed.
- [13] L. V. Keldysh, Zh. Eksp. Teor. Fiz. **47**, 1945 (1964) [Sov. Phys. JETP **20**, 1307 (1965)].
- [14] H. R. Reiss, Phys. Rev. A **22**, 1786 (1980).
- [15] C. Cohen-Tannoudji, J. Dupont-Roc, and G. Grynberg, *Atom-Photon Interaction* (Wiley, New York, 2004), p. 460.
- [16] For a review of physical aspects, L. Landau and E. Lifschitz, *Mechanics* (Pergamon, New York, 1960), p. 80; for a review of mathematical aspects, H. Hochstadt, *Differential Equations* (Dover, New York, 1963).
- [17] M. Yoshimura, in *Proceedings of the Symposium on Frontiers in Quantum Field Theory, Osaka, 1995* (World Scientific, Singapore, 1996).
- [18] M. Yoshimura, Prog. Theor. Phys. **94**, 873 (1995); H. Fujisaki, K. Kumekawa, M. Yamaguchi, and M. Yoshimura, Phys. Rev. D **53**, 6805 (1996); **54**, 2494 (1996).
- [19] H. Fujisaki, K. Kumekawa, M. Yamaguchi, and M. Yoshimura, Phys. Rev. D **53**, 6805 (1996).

- [20] Any complete theory satisfies the unitarity automatically. Our treatment of the microwave irradiation as externally given is however incomplete. The argument presented here, in particular, the inequality (146), is the limit that must be satisfied by any incomplete theory that treats the periodic external field as in our model.
- [21] The author would like to thank N. Sasao for a comment related to this problem.
- [22] H. A. Bethe and E. E. Salpeter, *Quantum Mechanics of One- and Two-Electron Atoms* (Plenum, New York, 1977).
- [23] M. Gavrilă and J. Z. Kaminski, Phys. Rev. Lett. **52**, 613 (1984); M. Pont, N. R. Walet, and M. Gavrilă, Phys. Rev. A **41**, 477 (1990); M. Pont, Phys. Rev. A **40**, 5659 (1989); M. Pont and M. Gavrilă, Phys. Rev. Lett. **65**, 2362 (1990).
- [24] Toru Takahashi and M. Yoshimura, arXiv:hep-ph/0703019.